



memorandum

CTAMOP,
School of Mathematics and Physics

To/MS: Distribution
From/MS: G. S. J. Armstrong, D. Clarke
Phone/FAX: 5-8236/606-0917
Email: gregorya@lanl.gov
Symbol: T-1:14-YYYYYY
Date: February 13, 2018

An RMT code for atoms in arbitrarily-polarized laser fields

I. Introduction

This memo describes several aspects of the time-dependent R -matrix code for atoms in arbitrarily-polarized laser fields.

II. Inner region

Solve

$$i \frac{\partial}{\partial t} \Psi_I(\mathbf{X}_{N+1}, t) = H_I(t) \Psi_I(\mathbf{X}_{N+1}, t) - \mathcal{L}_{N+1} \Psi(\mathbf{X}_{N+1}, t), \quad (1)$$

where

$$H_I(t) = H_{N+1} + \mathcal{L}_{N+1} + D_{N+1}(t). \quad (2)$$

Projecting onto eigenstates ψ_k we obtain the evolution equations for the time-dependent coefficients $C_k(t)$:

$$i \frac{d}{dt} C_k(t) = \sum_{k'} H_{I_{kk'}} C_{k'}(t) - \langle \psi_k | \mathcal{L}_{N+1} | \Psi \rangle, \quad (3)$$

which ultimately becomes

$$\frac{d}{dt} C_k(t) = -i \sum_{k'} H_{I_{kk'}} C_{k'}(t) + \left. \frac{1}{2} i \sum_p \omega_{pk} \frac{\partial f_p(r, t)}{\partial r} \right|_{r=b}, \quad (4)$$

where

$$f_p(r, t) = \langle \bar{\Phi}_p r_{N+1}^{-1} | \Psi \rangle_{r_{N+1}=r}, \quad (5)$$

and

$$\omega_{pk} = \langle \bar{\Phi}_p r_{N+1}^{-1} | \psi_k \rangle_{r_{N+1}=b}. \quad (6)$$

In matrix form, this inhomogeneous TDSE is given by

$$\frac{d}{dt} \mathbf{C} = -i \mathbf{H}_I(t) \mathbf{C}(t) + i \mathbf{S}(t), \quad (7)$$

with

$$S_k(t) = \frac{1}{2} \sum_p \omega_{pk} \left. \frac{\partial f_p(r, t)}{\partial r} \right|_{r=b}, \quad (8)$$

III. Outer region

$(N + 1)$ -electron wavefunction given by

$$\Psi(\mathbf{X}_{N+1}, t) = \sum_p \bar{\Phi}_p(\mathbf{X}_N; \hat{\mathbf{r}}_{N+1}, \sigma_{N+1}) \frac{1}{r} f_p(r, t). \quad (9)$$

Solve

$$i \frac{\partial}{\partial t} f_p(r, t) = h_{II_p}(r) f_p(r, t) + \sum_{p'} \left[W_{E_{pp'}}(r) + W_{D_{pp'}}(t) + W_{P_{pp'}}(r, t) \right] f_{p'}(r, t), \quad (10)$$

where

$$h_{II_p}(r) = -\frac{1}{2} \frac{d^2}{dr^2} + \frac{l_p(l_p + 1)}{2r^2} - \frac{Z - N}{r} + E_p, \quad (11)$$

$$W_{E_{pp'}}(r) = \left\langle \bar{\Phi}_p \left| \sum_{j=1}^N \frac{1}{|\mathbf{r} - \mathbf{r}_j|} - \frac{N}{r} \right| \bar{\Phi}_{p'} \right\rangle, \quad (12)$$

$$W_{D_{pp'}}(t) = \left\langle \bar{\Phi}_p \left| \mathbf{E}(t) \cdot \sum_{j=1}^N \mathbf{r}_j \right| \bar{\Phi}_{p'} \right\rangle, \quad (13)$$

$$W_{P_{pp'}}(r, t) = \langle \bar{\Phi}_p | \mathbf{E}(t) \cdot \mathbf{r} | \bar{\Phi}_{p'} \rangle. \quad (14)$$

IV. Electric field

The form of the electric field for linear polarization is

$$\mathbf{E}(t) = E_0 f(t) \cos(\omega t + \varphi) \mathbf{z}, \quad (15)$$

with $f(t)$ the pulse envelope, ω the frequency and φ the CEP.

For circular polarization, of helicity $\eta = \pm 1$, the field is

$$\mathbf{E}(t) = \frac{1}{\sqrt{2}} E_0 f(t) [\cos(\omega t + \varphi) \mathbf{x} + \eta \sin(\omega t + \varphi) \mathbf{y}]. \quad (16)$$

For elliptical polarization (ellipticity ϵ) in the xy plane, we have

$$\mathbf{E}(t) = E_0 f(t) \frac{1}{\sqrt{1 + \epsilon^2}} [\cos(\omega t + \varphi) \mathbf{x} + \epsilon \sin(\omega t + \varphi) \mathbf{y}]. \quad (17)$$

Special cases are $\epsilon = 0$ (linear) and $\epsilon = \pm 1$ (circular, with $\eta = \epsilon$).

V. Matrix elements

A. The W_D term

Using

$$\bar{\Phi}_p = \textcolor{red}{r_{N+1}^{-1}} |\alpha_i L_i l_i LM_L\rangle |S_i \frac{1}{2} S M_S\rangle, \quad (18)$$

the W_D term is given by

$$W_{D_{pp'}}(t) = E(t) \delta_{SS'} \delta_{S_i S'_i} \delta_{M_S M'_S} \delta_{M_{S_i} M'_{S_i}} \sum_{j=1}^N r_j \langle \alpha_i L_i l_i LM_L | \cos \theta_j | \alpha'_i L'_i l'_i L' M'_L \rangle, \quad (19)$$

where we use the Fano-Racah phase convention, so that

$$D_N = \mathbf{E}(t) \cdot \sum_{j=1}^N \mathbf{r}_j = E(t) \sum_{j=1}^N z_j = -i E(t) \sum_{j=1}^N T_0^{(1)}(r_j, \theta_j, \phi_j), \quad (20)$$

where $T_0^{(1)}(r_j, \theta_j, \phi_j) = \sqrt{\frac{4\pi}{3}} r_j Y_{10}^{Fano-Racah}(\theta_j, \phi_j) = ir_j \cos \theta_j$ is a spherical tensor. Now, the Wigner-Eckardt theorem (Eq. (5.64) in [2]),

$$\langle \alpha_i L_i l_i LM_L | T_0^{(1)} | \alpha'_i L'_i l'_i L' M'_L \rangle = (-1)^{L-M_L} \delta_{M_L, M'_L} \begin{pmatrix} L & 1 & L' \\ -M_L & 0 & M_L \end{pmatrix} \langle \alpha_i L_i l_i L \| T^1 \| \alpha'_i L'_i l'_i L' \rangle. \quad (21)$$

With

$$\langle \alpha_i L_i l_i L \| T^1 \| \alpha'_i L'_i l'_i L' \rangle = \delta_{l_i l'_i} (-1)^{L_i + l_i + L' + 1} \sqrt{(2L+1)(2L'+1)} \left\{ \begin{array}{ccc} L_i & L & l_i \\ L' & L'_i & 1 \end{array} \right\} \langle \alpha_i L_i \| T^1 \| \alpha'_i L'_i \rangle \quad (22)$$

this reduces to

$$W_{D_{pp'}}(t) = \delta_{SS'} \delta_{S_i S'_i} \delta_{M_S M'_S} \delta_{M_{S_i} M'_{S_i}} (-1)^{L-M_L+L_i+l_i+L'+1} \sqrt{(2L+1)(2L'+1)} \times \delta_{l_i l'_i} \delta_{M_L M'_L} \langle \alpha_i L_i \| D_N \| \alpha'_i L'_i \rangle \begin{pmatrix} L & 1 & L' \\ -M_L & 0 & M_L \end{pmatrix} \left\{ \begin{array}{ccc} L_i & L & l_i \\ L' & L'_i & 1 \end{array} \right\}, \quad (23)$$

which may be simplified by an odd permutation of the 3-j symbol columns, incurring a phase of $(-1)^{L+L'+1}$, and modifying the 6-j symbol entries, so that

$$W_{D_{pp'}}(t) = \delta_{SS'} \delta_{S_i S'_i} \delta_{M_S M'_S} \delta_{M_{S_i} M'_{S_i}} (-1)^{-M_L+L_i+l_i} \sqrt{(2L+1)(2L'+1)} \times \delta_{l_i l'_i} \delta_{M_L M'_L} \langle \alpha_i L_i \| D_N \| \alpha'_i L'_i \rangle \begin{pmatrix} L & L' & 1 \\ -M_L & M_L & 0 \end{pmatrix} \left\{ \begin{array}{ccc} L & L' & 1 \\ L'_i & L_i & l_i \end{array} \right\}. \quad (24)$$

Writing out D_N explicitly, we have that

$$W_{D_{pp'}}(t) = E(t)\delta_{SS'}\delta_{S_i S'_i}\delta_{M_S M'_S}\delta_{M_{S_i} M'_{S_i}}(-1)^{-M_L + L_i + l_i}\sqrt{(2L+1)(2L'+1)} \\ \times \delta_{l_i l'_i}\delta_{M_L M'_L}\sum_{j=1}^N \langle \alpha_i L_i \| r_j \cos \theta_j \| \alpha'_i L'_i \rangle \begin{pmatrix} L & L' & 1 \\ -M_L & M_L & 0 \end{pmatrix} \left\{ \begin{array}{ccc} L & L' & 1 \\ L'_i & L_i & l_i \end{array} \right\}. \quad (25)$$

A.1. Comparison with original result

Original form given in [1] is

$$W_{D_{pp'}}(t) = (-1)^{L_i + L'_i + 1}\sqrt{(2L'+1)}(10L'M_L|LM_L)W(1L'_i Ll_i; L_i L') \\ \times \langle \Phi_i \| D_N \| \Phi_{i'} \rangle \delta_{SS'}\delta_{S_i S'_i}\delta_{M_S M'_S}\delta_{M_{S_i} M'_{S_i}}\delta_{M_L M'_L}\delta_{l_i l'_i}, \quad (26)$$

Changing to 3-j and 6-j symbols, using

$$(j_1 m_1 j_2 m_2 | JM) = (-1)^{j_2 - j_1 - M}\sqrt{2J+1} \begin{pmatrix} j_1 & j_2 & J \\ m_1 & m_2 & -M \end{pmatrix}, \quad (27)$$

$$W(j_1 j_2 J j_3, J_{12} J_{23}) = (-1)^{j_1 + j_2 + j_3 + J} \left\{ \begin{array}{ccc} j_1 & j_2 & J_{12} \\ j_3 & J & J_{23} \end{array} \right\}, \quad (28)$$

and writing $|\Phi_i\rangle = |\alpha_i L_i\rangle$ in the reduced matrix element, gives

$$W_{D_{pp'}}(t) = (-1)^{L_i + L'_i + 1}\sqrt{(2L'+1)(2L+1)}(-1)^{L'-1-M_L} \begin{pmatrix} 1 & L' & L \\ 0 & M_L & -M_L \end{pmatrix} \\ \times (-1)^{1+L'_i+L+l_i} \left\{ \begin{array}{ccc} 1 & L'_i & L_i \\ l_i & L & L' \end{array} \right\} \langle \alpha_i L_i \| D_N \| \alpha'_i L'_i \rangle \delta_{SS'}\delta_{S_i S'_i}\delta_{M_S M'_S}\delta_{M_{S_i} M'_{S_i}}\delta_{M_L M'_L}\delta_{l_i l'_i}. \quad (29)$$

Now some phase factors cancel, so that

$$(-1)^{L_i + L'_i + 1 + (L'-1-M_L) + (1+L'_i+L+l_i)} = (-1)^{L_i + L' + 1 - M_L + L + l_i} \quad (30)$$

and so

$$W_{D_{pp'}}(t) = (-1)^{L_i + L' + 1 - M_L + L + l_i}\sqrt{(2L'+1)(2L+1)} \begin{pmatrix} 1 & L' & L \\ 0 & M_L & -M_L \end{pmatrix} \\ \times \left\{ \begin{array}{ccc} 1 & L'_i & L_i \\ l_i & L & L' \end{array} \right\} \langle \alpha_i L_i \| D_N \| \alpha'_i L'_i \rangle \delta_{SS'}\delta_{S_i S'_i}\delta_{M_S M'_S}\delta_{M_{S_i} M'_{S_i}}\delta_{M_L M'_L}\delta_{l_i l'_i}. \quad (31)$$

Now using

$$\begin{pmatrix} 1 & L' & L \\ 0 & M_L & -M_L \end{pmatrix} = (-1)^{L+L'+1} \begin{pmatrix} L & L' & 1 \\ -M_L & M_L & 0 \end{pmatrix} \quad (32)$$

and

$$\left\{ \begin{array}{ccc} 1 & L'_i & L_i \\ l_i & L & L' \end{array} \right\} = \left\{ \begin{array}{ccc} L & L' & 1 \\ L'_i & L_i & l_i \end{array} \right\}, \quad (33)$$

then we have

$$W_{D_{pp'}}(t) = (-1)^{L_i-M_L+l_i} \sqrt{(2L'+1)(2L+1)} \begin{pmatrix} L & L' & 1 \\ -M_L & M_L & 0 \end{pmatrix} \left\{ \begin{array}{ccc} L & L' & 1 \\ L'_i & L_i & l_i \end{array} \right\} \times \langle \alpha_i L_i \| D_N \| \alpha'_i L'_i \rangle \delta_{SS'} \delta_{S_i S'_i} \delta_{M_S M'_S} \delta_{M_{S_i} M'_{S_i}} \delta_{M_L M'_L} \delta_{l_i l'_i}, \quad (34)$$

which is the same Eq. (24) — middle 3-j symbol undergoes column swap and bottom row sign change, so no extra phase occurs, column swaps in 6-j symbol incur no phase, so phases should be the same in both expressions. Factors of i are in the reduced matrix element in the original expression.

A.2. Other polarizations

To account for other polarizations, Eq. (21) must be modified, so that

$$\langle \alpha_i L_i l_i LM_L | T_1^{(1)} | \alpha'_i L'_i l'_i L' M'_L \rangle = (-1)^{L-M_L} \delta_{M_L, M'_L + 1} \begin{pmatrix} L & 1 & L' \\ -M_L & 1 & M'_L \end{pmatrix} \langle \alpha_i L_i l_i L \| T^1 \| \alpha'_i L'_i l'_i L' \rangle, \quad (35)$$

and

$$\langle \alpha_i L_i l_i LM_L | T_{-1}^{(1)} | \alpha'_i L'_i l'_i L' M'_L \rangle = (-1)^{L-M_L} \delta_{M_L, M'_L - 1} \begin{pmatrix} L & 1 & L' \\ -M_L & -1 & M'_L \end{pmatrix} \langle \alpha_i L_i l_i L \| T^1 \| \alpha'_i L'_i l'_i L' \rangle. \quad (36)$$

These expressions differ only in the 3-j symbol coupling M_L and M'_L . Therefore, the μ -component of W_D ($W_D^{(\mu)}$) takes the general form (CHECK!!!)

$$W_{D_{pp'}}^{(\mu)}(t) = E_\mu(t) \delta_{SS'} \delta_{S_i S'_i} \delta_{M_S M'_S} \delta_{M_{S_i} M'_{S_i}} (-1)^{-M_L+L_i+l_i} \sqrt{(2L+1)(2L'+1)} \times \delta_{l_i l'_i} \delta_{M_L M'_L + \mu} \sum_{j=1}^N \langle \alpha_i L_i \| T^{(1)}(r_j, \theta_j) \| \alpha'_i L'_i \rangle \begin{pmatrix} L & L' & 1 \\ -M_L & M'_L & \mu \end{pmatrix} \left\{ \begin{array}{ccc} L & L' & 1 \\ L'_i & L_i & l_i \end{array} \right\}. \quad (37)$$

The original expression may be generalized to the form (CHECK!!!!)

$$W_{D_{pp'}}^{(\mu)}(t) = E_\mu(t) (-1)^{L_i+L'_i+1} \sqrt{(2L'+1)} (1\mu L' M'_L | LM_L) W(1L'_i L l_i; L_i L') \times \sum_{j=1}^N \langle \Phi_i \| T^{(1)}(r_j, \theta_j) \| \Phi_{i'} \rangle \delta_{SS'} \delta_{S_i S'_i} \delta_{M_S M'_S} \delta_{M_{S_i} M'_{S_i}} \delta_{l_i l'_i} \delta_{M_L M'_L + \mu}, \quad (38)$$

VI. Summary of W_D matrix elements for different polarizations

A. Spherical components (CHECK D_N DEFINITION)

Eq. (35) may be generalized to give

$$\langle \alpha_i L_i l_i LM_L | T_1^{(\mu)} | \alpha'_i L'_i l'_i L' M'_L \rangle = (-1)^{L-M_L} \delta_{M_L, M'_L + \mu} \begin{pmatrix} L & 1 & L' \\ -M_L & \mu & M'_L \end{pmatrix} \langle \alpha_i L_i l_i L \| T^1 \| \alpha'_i L'_i l'_i L' \rangle, \quad (39)$$

or using Clebsch-Gordan and Racah coefficients,

$$\langle \alpha_i L_i l_i LM_L | T_1^{(\mu)} | \alpha'_i L'_i l'_i L' M'_L \rangle = \delta_{M_L, M'_L + \mu} \frac{1}{\sqrt{2L'+1}} \langle 1\mu L' M'_L | LM_L \rangle \langle \alpha_i L_i l_i L \| T^1 \| \alpha'_i L'_i l'_i L' \rangle, \quad (40)$$

and using Eq. (22),

$$\langle \alpha_i L_i l_i L \| T^1 \| \alpha'_i L'_i l'_i L' \rangle = \delta_{l_i l'_i} (-1)^{L_i + L'_i + 1} \sqrt{(2L+1)(2L'+1)} W(1l_i LL'_i, L_i L') \langle \alpha_i L_i \| T^1 \| \alpha'_i L'_i \rangle, \quad (41)$$

we then have that

$$\boxed{\langle \alpha_i L_i l_i LM_L | T_1^{(\mu)} | \alpha'_i L'_i l'_i L' M'_L \rangle = \delta_{l_i l'_i} (-1)^{L_i + L'_i + 1} \sqrt{2L+1} W(1l_i LL'_i, L_i L') \langle \alpha_i L_i \| T^1 \| \alpha'_i L'_i \rangle \times \delta_{M_L, M'_L + \mu} \langle 1\mu L' M'_L | LM_L \rangle. \quad (42)}$$

Therefore, the W_D interaction Hamiltonian has three terms, $\mu = -1, 0, 1$, where

$$W_{D_{pp'}}^{(\mu)} = E_\mu(t) \langle \alpha_i L_i l_i LM_L | D_N | \alpha'_i L'_i l'_i L' M'_L \rangle, \quad (43)$$

where the -1,0,1 components are

$$\boxed{W_{D_{pp'}}^{(-1)} = (-1)^{L_i + L'_i + 1} \sqrt{2L'+1} W(1L'_i Ll_i, L_i L') (1 - 1L' M'_L | LM_L) \delta_{M_L, M'_L - 1} \times \langle \alpha_i L_i \| D_N \| \alpha'_i L'_i \rangle \delta_{SS'} \delta_{S_i S'_i} \delta_{MSM'_S} \delta_{MS_i M'_{S_i}}, \quad (44)}$$

$$\boxed{W_{D_{pp'}}^{(0)} = (-1)^{L_i + L'_i + 1} \sqrt{2L'+1} W(1L'_i Ll_i, L_i L') (10L' M'_L | LM_L) \delta_{M_L, M'_L} \times \langle \alpha_i L_i \| D_N \| \alpha'_i L'_i \rangle \delta_{SS'} \delta_{S_i S'_i} \delta_{MSM'_S} \delta_{MS_i M'_{S_i}}, \quad (45)}$$

$$\boxed{W_{D_{pp'}}^{(+1)} = (-1)^{L_i + L'_i + 1} \sqrt{2L'+1} W(1L'_i Ll_i, L_i L') (1 + 1L' M'_L | LM_L) \delta_{M_L, M'_L + 1} \times \langle \alpha_i L_i \| D_N \| \alpha'_i L'_i \rangle \delta_{SS'} \delta_{S_i S'_i} \delta_{MSM'_S} \delta_{MS_i M'_{S_i}}. \quad (46)}$$

B. Cartesian components (CHECK!!!!)

Using

$$x = -i \frac{1}{\sqrt{2}} (r_{-1}^{(1)} - r_1^{(1)}), \quad (47)$$

$$y = \frac{1}{\sqrt{2}} (r_{-1}^{(1)} + r_1^{(1)}), \quad (48)$$

$$z = -ir_0. \quad (49)$$

for x -axis polarization we have

$$\begin{aligned} W_{D_{pp'}}^{(x)} &= -i(-1)^{L_i+L'_i+1} \sqrt{\frac{2L'+1}{2}} W(1L'_i Ll_i, L_i L') r \langle \alpha_i L_i \| D_N \| \alpha'_i L'_i \rangle \\ &\times [(1 - 1L'M'_L | LM_L) \delta_{M_L, M'_L - 1} - (11L'M'_L | LM_L) \delta_{M_L, M'_L + 1}] \\ &\times \delta_{SS'} \delta_{S_i S'_i} \delta_{M_S M'_S} \delta_{M_{S_i} M'_{S_i}} \end{aligned} \quad (50)$$

for y -axis polarization we have

$$\begin{aligned} W_{D_{pp'}}^{(y)} &= (-1)^{L_i+L'_i+1} \sqrt{\frac{2L'+1}{2}} W(1L'_i Ll_i, L_i L') r \langle \alpha_i L_i \| D_N \| \alpha'_i L'_i \rangle \\ &\times [(1 - 1L'M'_L | LM_L) \delta_{M_L, M'_L - 1} + (11L'M'_L | LM_L) \delta_{M_L, M'_L + 1}] \\ &\times \delta_{SS'} \delta_{S_i S'_i} \delta_{M_S M'_S} \delta_{M_{S_i} M'_{S_i}}, \end{aligned} \quad (51)$$

for z -axis polarization we have

$$\begin{aligned} W_{D_{pp'}}^{(z)} &= -i(-1)^{L_i+L'_i+1} \sqrt{(2L'+1)} W(1L'_i Ll_i, L_i L') r \langle \alpha_i L_i \| D_N \| \alpha'_i L'_i \rangle \\ &\times (10L'M'_L | LM_L) \delta_{M_L, M'_L} \\ &\times \delta_{SS'} \delta_{S_i S'_i} \delta_{M_S M'_S} \delta_{M_{S_i} M'_{S_i}}. \end{aligned} \quad (52)$$

C. The W_P term

We may write the angular part of the residual ion states explicitly, so that

$$\bar{\Phi}_p = |\alpha_i L_i l_i LM_L\rangle |S_i \frac{1}{2} S M_S\rangle. \quad (53)$$

The W_P coupling between the laser and outgoing electron is then given by

$$W_{P_{pp'}}(t) = E(t) r \delta_{SS'} \delta_{S_i S'_i} \delta_{M_S M'_S} \delta_{M_{S_i} M'_{S_i}} \langle \alpha_i L_i l_i LM_L | \cos \theta | \alpha'_i L'_i l'_i L' M'_L \rangle, \quad (54)$$

C.1. Derivation 1: Analogy with HELIUM angular matrix elements

In [3], angular matrix elements for helium were derived for non-zero M . These may be generalized and adapted to the Fano-Racah phase convention to give the corresponding expression for W_P .

In the case of helium, using the Condon-Shortley phase convention, Karen gives in Eq. (B.11) of [3]

$$\begin{aligned} \langle l_1 l_2 LM | \cos \theta_1 | l'_1 l'_2 L' M' \rangle &= (-1)^{l_2 - M_L} \sqrt{(2L+1)(2L'+1)(2l_1+1)(2l'_1+1)} \\ &\times \delta_{l_2 l'_2} \delta_{M M'} \left(\begin{array}{ccc} l_1 & 1 & l'_1 \\ 0 & 0 & 0 \end{array} \right) \left(\begin{array}{ccc} L & L' & 1 \\ -M & M & 0 \end{array} \right) \left\{ \begin{array}{ccc} L & L' & 1 \\ l'_1 & l_1 & l_2 \end{array} \right\}. \end{aligned} \quad (55)$$

Note here that primed and unprimed quantum numbers have been swapped relative to Eq. (B.11) of [3] to give the form used in this work (i.e. primes on right not left).

We may apply this to derive W_P by first noting that

$$|\alpha_i L_i l_i LM_L\rangle = (-1)^{l_i + L_i + L} |l_i \alpha_i L_i LM_L\rangle, \quad (56)$$

so that

$$\begin{aligned} \langle \alpha_i L_i l_i LM_L | \cos \theta | \alpha'_i L'_i l'_i L' M'_L \rangle &= (-1)^{l_i + L_i + L + l'_i + L'_i + L'} \langle l_i \alpha_i L_i LM_L | \cos \theta | l'_i \alpha'_i L'_i L' M'_L \rangle, \\ &= (-1)^{L + L' + 1} \langle l_i \alpha_i L_i LM_L | \cos \theta | l'_i \alpha'_i L'_i L' M'_L \rangle, \end{aligned} \quad (57)$$

since $L_i = L'_i$ and $l_i + l'_i$ is odd.

At this point, Eq. (55) can be used directly to give $\langle l_i \alpha_i L_i LM_L | \cos \theta | l'_i \alpha'_i L'_i L' M'_L \rangle$ (noting the order of the angular momenta being coupled).

Using the expression given in [3] together with the Fano-Racah phase convention (Condon-Shortley convention used in [3]),

$$\begin{aligned} \langle \alpha_i L_i l_i LM_L | \cos \theta | \alpha'_i L'_i l'_i L' M'_L \rangle &= i^{l'_i - l_i} (-1)^{L+L'+1+L_i-M_L} \sqrt{(2L+1)(2L'+1)(2l_i+1)(2l'_i+1)} \\ &\times \delta_{\alpha_i \alpha'_i} \delta_{L_i L'_i} \delta_{M_L M'_L} \left(\begin{array}{ccc} l_i & 1 & l'_i \\ 0 & 0 & 0 \end{array} \right) \left(\begin{array}{ccc} L & L' & 1 \\ -M_L & M_L & 0 \end{array} \right) \left\{ \begin{array}{ccc} L & L' & 1 \\ l'_i & l_i & L_i \end{array} \right\}, \end{aligned} \quad (58)$$

and so

$$\begin{aligned} W_{P_{pp'}}(t) &= E(t) r \delta_{SS'} \delta_{S_i S'_i} \delta_{M_S M'_S} \delta_{M_{S_i} M'_{S_i}} i^{l'_i - l_i} (-1)^{L+L'+1+L_i-M_L} \sqrt{(2L+1)(2L'+1)(2l_i+1)(2l'_i+1)} \\ &\times \delta_{\alpha_i \alpha'_i} \delta_{L_i L'_i} \delta_{M_L M'_L} \left(\begin{array}{ccc} l_i & 1 & l'_i \\ 0 & 0 & 0 \end{array} \right) \left(\begin{array}{ccc} L & L' & 1 \\ -M_L & M_L & 0 \end{array} \right) \left\{ \begin{array}{ccc} L & L' & 1 \\ l'_i & l_i & L_i \end{array} \right\}. \end{aligned} \quad (59)$$

C.2. Comparison with original result

Original result, from [1], is

$$\begin{aligned} W_{P_{pp'}} &= iE(t)(-1)^{L+L'} \sqrt{(2l'_i+1)(2L+1)} (LM_L 10 | L'M_L) \frac{a(l'_i)}{(l_i 010 | l'_i 0)} W(1l'_i LL_i, l_i L') \\ &\times r \delta_{SS'} \delta_{S_i S'_i} \delta_{M_S M'_S} \delta_{M_{S_i} M'_{S_i}} \delta_{L_i, L'_i} \delta_{M_{L_i}, M'_{L_i}} \delta_{\alpha_i, \alpha'_i}, \end{aligned} \quad (60)$$

with

$$a(l'_i) = \left\{ \begin{array}{ll} \frac{l'_i}{\sqrt{(2l'_i-1)(2l'_i+1)}} & l_i = l'_i - 1 \\ -\frac{l'_i}{\sqrt{(2l'_i+1)(2l'_i+3)}} & l_i = l'_i + 1 \end{array} \right\} = i^{l'_i - l_i - 1} \sqrt{(2l_i+1)(2l'_i+1)} \left(\begin{array}{ccc} l_i & 1 & l'_i \\ 0 & 0 & 0 \end{array} \right)^2. \quad (61)$$

Now we attempt to write the original expression in terms of 3-j and 6-j symbols, using

$$(j_1 m_1 j_2 m_2 | JM) = (-1)^{j_2 - j_1 - M} \sqrt{2J+1} \left(\begin{array}{ccc} j_1 & j_2 & J \\ m_1 & m_2 & -M \end{array} \right), \quad (62)$$

$$W(j_1 j_2 J j_3, J_{12} J_{23}) = (-1)^{j_1 + j_2 + j_3 + J} \left\{ \begin{array}{ccc} j_1 & j_2 & J_{12} \\ j_3 & J & J_{23} \end{array} \right\}. \quad (63)$$

Then, the original result becomes

$$W_{P_{pp'}} = iE(t)(-1)^{L+L'}\sqrt{(2l'_i+1)(2L+1)}(-1)^{1-L-M_L}\sqrt{2L'+1}\begin{pmatrix} L & 1 & L' \\ M_L & 0 & -M_L \end{pmatrix} \\ \times \frac{i^{l'_i-l_i-1}\sqrt{(2l_i+1)(2l'_i+1)}}{(-1)^{l_i-1}\sqrt{2l'_i+1}} \begin{pmatrix} l_i & 1 & l'_i \\ 0 & 0 & 0 \end{pmatrix}^2 (-1)^{1+l'_i+L_i+L} \left\{ \begin{array}{ccc} 1 & l'_i & l_i \\ L_i & L & L' \end{array} \right\} \\ \times r\delta_{SS'}\delta_{S_i S'_i}\delta_{M_S M'_S}\delta_{M_{S_i} M'_{S_i}}\delta_{L_i L'_i}\delta_{M_{L_i} M'_{L_i}}\delta_{\alpha_i \alpha'_i}. \quad (64)$$

Now, many phase factors cancel, so that

$$(-1)^{L+L'+(1-L-M_L)+(1+l'_i+L_i+L)-(l_i-1)} = (-1)^{L+L'-M_L+l'_i-(l_i-1)+L_i} = (-1)^{L+L'-M_L+L_i}, \quad (65)$$

since $l'_i - (l_i - 1)$ is always even.

Making this simplification, and cancelling factor in the ratio term, the expression simplifies to

$$W_{P_{pp'}} = iE(t)(-1)^{L+L'-M_L+L_i}\sqrt{(2l'_i+1)(2L+1)}\sqrt{2L'+1}\begin{pmatrix} L & 1 & L' \\ M_L & 0 & -M_L \end{pmatrix} \\ \times i^{l'_i-l_i-1}\sqrt{(2l_i+1)} \begin{pmatrix} l_i & 1 & l'_i \\ 0 & 0 & 0 \end{pmatrix} \left\{ \begin{array}{ccc} 1 & l'_i & l_i \\ L_i & L & L' \end{array} \right\} \\ \times r\delta_{SS'}\delta_{S_i S'_i}\delta_{M_S M'_S}\delta_{M_{S_i} M'_{S_i}}\delta_{L_i L'_i}\delta_{M_{L_i} M'_{L_i}}\delta_{\alpha_i \alpha'_i}. \quad (66)$$

Now, both the first 3-j symbol and the 6-j symbol need to be modified to agree with Eq. (59). The 3-j symbol requires two modifications: an uneven permutation of columns, so that the top row becomes $L, L', 1$, and a multiplication of the bottom row elements by -1 so that the bottom row becomes $-M_L, M_L, 0$. Both these changes incur a phase factor $(-1)^{L+L'+1}$, and so that

$$\begin{pmatrix} L & 1 & L' \\ M_L & 0 & -M_L \end{pmatrix} = \begin{pmatrix} L & L' & 1 \\ -M_L & M_L & 0 \end{pmatrix}. \quad (67)$$

The 6-j symbol also requires swapping of entires, which do not incur additional phases, so that

$$\left\{ \begin{array}{ccc} 1 & l'_i & l_i \\ L_i & L & L' \end{array} \right\} = \left\{ \begin{array}{ccc} 1 & L & L' \\ L_i & l'_i & l_i \end{array} \right\} = \left\{ \begin{array}{ccc} L & L' & 1 \\ l'_i & l_i & L_i \end{array} \right\}. \quad (68)$$

After these changes, W_P becomes

$$\begin{aligned}
 W_{P_{pp'}} &= i^{l'_i - l_i} E(t) (-1)^{L+L'+L_i-M_L} \sqrt{(2l'_i + 1)(2L + 1)(2L' + 1)(2l_i + 1)} \\
 &\times \begin{pmatrix} l_i & 1 & l'_i \\ 0 & 0 & 0 \end{pmatrix} \begin{pmatrix} L & L' & 1 \\ -M_L & M_L & 0 \end{pmatrix} \left\{ \begin{array}{ccc} L & L' & 1 \\ l'_i & l_i & L_i \end{array} \right\} \\
 &\times r \delta_{SS'} \delta_{S_i S'_i} \delta_{M_S M'_S} \delta_{M_{S_i} M'_{S_i}} \delta_{L_i L'_i} \delta_{M_{L_i} M'_{L_i}} \delta_{\alpha_i \alpha'_i}. \quad (69)
 \end{aligned}$$

This appears to differ from the result of (59) by a factor of -1.

C.3. Daniel's derivation and minus sign

Starting from Daniel's Eq. (1) is (writing out $|L\rangle$ as $|\alpha_i L_i l_i L M_L\rangle$ from Eq. (53))

$$\langle \alpha_i L_i l_i L M_L | \hat{\epsilon} \cdot \mathbf{r} | \alpha'_i L'_i l'_i L' M'_L \rangle = -i(-1)^{L+L'} \frac{1}{\sqrt{2L'+1}} (LM_L 10 | L' M_L \rangle \langle \alpha_i L_i l_i L \| r^{(1)} \| \alpha'_i L'_i l'_i L' \rangle), \quad (70)$$

where $r^{(1)} = r \sqrt{\frac{4\pi}{3}} Y_{10}^{Fano-Racah}(\theta, \phi) = ir \cos \theta$, and Eq. (2) gives the reduced matrix element

$$\langle \alpha_i L_i l_i L \| r^{(1)} \| \alpha'_i L'_i l'_i L' \rangle = \sqrt{2L+1} \sqrt{2L'+1} W(1l'_i LL_i; l_i L') \langle l_i \| r^{(1)} \| l'_i \rangle \delta_{\alpha_i \alpha'_i} \delta_{L_i L'_i}. \quad (71)$$

Daniel derives the reduced matrix element from the full reduced matrix element. Equivalently, the uncoupled reduced matrix element $\langle l_i \| r^{(1)} \| l'_i \rangle$ can be evaluated directly as

$$\langle l_i \| r^{(1)} \| l'_i \rangle = i^{l'_i + 1 - l_i} (-1)^{l_i} \sqrt{(2l_i + 1)(2l'_i + 1)} \begin{pmatrix} l_i & 1 & l'_i \\ 0 & 0 & 0 \end{pmatrix} r. \quad (72)$$

I could write this in terms of a Clebsch-Gordan coefficient, but as a test of phase factors I'm going to write it in terms of 3-j symbols times some phases. This means that Eq. (71) becomes

$$\langle \alpha_i L_i l_i L \| r^{(1)} \| \alpha'_i L'_i l'_i L' \rangle = \sqrt{[L][L'][l_i][l'_i]} W(1l'_i LL_i; l_i L') i^{l'_i + 1 - l_i} (-1)^{l_i} \begin{pmatrix} l_i & 1 & l'_i \\ 0 & 0 & 0 \end{pmatrix} r \delta_{\alpha_i \alpha'_i} \delta_{L_i L'_i}, \quad (73)$$

where $[L] = 2L + 1$.

Converting the Clebsch-Gordan coefficient to a 3-j symbol, I find

$$(LM_L 10 | L' M_L \rangle = (-1)^2 (-1)^{L'-M_L} \sqrt{2L'+1} \begin{pmatrix} L & L' & 1 \\ M_L & -M_L & 0 \end{pmatrix}, \quad (74)$$

so Eq. (70) becomes

$$\begin{aligned} \langle \alpha_i L_i l_i LM_L | \hat{\epsilon} \cdot \mathbf{r} | \alpha'_i L'_i l'_i L' M'_L \rangle &= -i(-1)^{L+L'} (-1)^2 (-1)^{L'-M_L} \begin{pmatrix} L & L' & 1 \\ M_L & -M_L & 0 \end{pmatrix} \\ &\times \sqrt{[L][L'][l_i][l'_i]} W(1l'_i LL_i; l_i L') i^{l'_i+1-l_i} (-1)^{l_i} \begin{pmatrix} l_i & 1 & l'_i \\ 0 & 0 & 0 \end{pmatrix} r \delta_{\alpha_i \alpha'_i} \delta_{L_i L'_i}, \end{aligned} \quad (75)$$

which simplifies to

$$\begin{aligned} \langle \alpha_i L_i l_i LM_L | \hat{\epsilon} \cdot \mathbf{r} | \alpha'_i L'_i l'_i L' M'_L \rangle &= i^{l'_i-l_i} (-1)^{L-M_L+l_i} \begin{pmatrix} L & L' & 1 \\ M_L & -M_L & 0 \end{pmatrix} \\ &\times \sqrt{[L][L'][l_i][l'_i]} W(1l'_i LL_i; l_i L') \begin{pmatrix} l_i & 1 & l'_i \\ 0 & 0 & 0 \end{pmatrix} r \delta_{\alpha_i \alpha'_i} \delta_{L_i L'_i}. \end{aligned} \quad (76)$$

I leave this expression in terms of the Racah W coefficient to avoid introducing yet more phases. Let's now compare the published expression with this (Daniel's) result.

In the original form,

$$\begin{aligned} W_{P_{pp'}} &= iE(t)(-1)^{L+L'} \sqrt{(2l'_i+1)(2L+1)} (LM_L 10 | L' M_L) \frac{a(l'_i)}{(l_i 010 | l'_i 0)} W(1l'_i LL_i, l_i L') \\ &\times r \delta_{SS'} \delta_{S_i S'_i} \delta_{M_S M'_S} \delta_{M_{S_i} M'_{S_i}} \delta_{L_i, L'_i} \delta_{M_{L_i}, M'_{L_i}} \delta_{\alpha_i, \alpha'_i}, \end{aligned} \quad (77)$$

so

$$\langle \alpha_i L_i l_i LM_L | \hat{\epsilon} \cdot \mathbf{r} | \alpha'_i L'_i l'_i L' M'_L \rangle = i(-1)^{L+L'} \sqrt{[l'_i][L]} (LM_L 10 | L' M_L) \frac{a(l'_i)}{(l_i 010 | l'_i 0)} W(1l'_i LL_i, l_i L') r \delta_{\alpha_i \alpha'_i} \delta_{L_i L'_i} \quad (78)$$

On pages 5-7 of his derivation, Daniel derives $a(l'_i)$ to be

$$ia(l'_i) = i^{l'_i-l_i} \sqrt{\frac{[l'_i]}{[l_i]}} (10l'_i 0 | l_i 0)^2.$$

(79)

Converting to 3-j symbols to test this against my result in Eq. (61), Daniel's result becomes

$$ia(l'_i) = i^{l'_i-l_i} \sqrt{\frac{[l'_i]}{[l_i]}} [l_i] \begin{pmatrix} l_i & 1 & l'_i \\ 0 & 0 & 0 \end{pmatrix}^2 = i^{l'_i-l_i} \sqrt{[l'_i][l_i]} \begin{pmatrix} l_i & 1 & l'_i \\ 0 & 0 & 0 \end{pmatrix}^2,$$

(80)

which is what I find in Eq. (61). Now we have that

$$(10l'_i 0 | l_i 0)^2 = \frac{[l_i]}{[l'_i]} (l_i 010 | l'_i 0)^2 \quad (81)$$

so that

$$\frac{ia(l'_i)}{(l_i010|l'_i0)} = i^{l'_i-l_i} \sqrt{\frac{[l_i]}{[l'_i]}} (l_i010|l'_i0) \quad (82)$$

So, the original derivation gives that

$$\begin{aligned} \langle \alpha_i L_i l_i L M_L | \hat{\epsilon} \cdot \mathbf{r} | \alpha'_i L'_i l'_i L' M'_L \rangle &= (-1)^{L+L'} \sqrt{[l'_i][L]} (L M_L 10 | L' M_L) i^{l'_i-l_i} \sqrt{\frac{[l_i]}{[l'_i]}} (l_i010|l'_i0) \\ &\quad \times W(1l'_i LL_i, l_i L') r \delta_{\alpha_i \alpha'_i} \delta_{L_i L'_i} \end{aligned} \quad (83)$$

which reduces to

$$\langle \alpha_i L_i l_i L M_L | \hat{\epsilon} \cdot \mathbf{r} | \alpha'_i L'_i l'_i L' M'_L \rangle = (-1)^{L+L'} \sqrt{[l_i][L]} (L M_L 10 | L' M_L) i^{l'_i-l_i} (l_i010|l'_i0) W(1l'_i LL_i, l_i L') r \delta_{\alpha_i \alpha'_i} \delta_{L_i L'_i} \quad (84)$$

Now using

$$(L M_L 10 | L' M_L) = (-1)^2 (-1)^{L'-M_L} \sqrt{2L'+1} \begin{pmatrix} L & L' & 1 \\ M_L & -M_L & 0 \end{pmatrix} \quad (85)$$

I find that

$$\begin{aligned} \langle \alpha_i L_i l_i L M_L | \hat{\epsilon} \cdot \mathbf{r} | \alpha'_i L'_i l'_i L' M'_L \rangle &= (-1)^{L+L'} \sqrt{[l_i][L]} (-1)^{L'-M_L} \sqrt{2L'+1} \begin{pmatrix} L & L' & 1 \\ M_L & -M_L & 0 \end{pmatrix} \\ &\quad \times i^{l'_i-l_i} (-1)^{l'_i} \sqrt{2l'_i+1} \begin{pmatrix} l_i & 1 & l'_i \\ 0 & 0 & 0 \end{pmatrix} W(1l'_i LL_i, l_i L') r \delta_{\alpha_i \alpha'_i} \delta_{L_i L'_i}, \end{aligned} \quad (86)$$

which reduces to

$$\begin{aligned} \langle \alpha_i L_i l_i L M_L | \hat{\epsilon} \cdot \mathbf{r} | \alpha'_i L'_i l'_i L' M'_L \rangle &= \sqrt{[l_i][l'_i][L][L']} (-1)^{L-M_L+l'_i} \begin{pmatrix} L & L' & 1 \\ M_L & -M_L & 0 \end{pmatrix} \\ &\quad \times i^{l'_i-l_i} \begin{pmatrix} l_i & 1 & l'_i \\ 0 & 0 & 0 \end{pmatrix} W(1l'_i LL_i, l_i L') r \delta_{\alpha_i \alpha'_i} \delta_{L_i L'_i}. \end{aligned} \quad (87)$$

Note the factor of $(-1)^{L-M_L+l'_i}$ here, compared to the factor $(-1)^{L-M_L+l_i}$ in Daniel's result of Eq. (76). All other factors are the same as in Eq. (76). Since $l'_i + l_i + 1$ must be even, then

$$(-1)^{L-M_L+l'_i} = -(-1)^{L-M_L+l_i}. \quad (88)$$

This seems to confirm Daniel's minus sign.

C.4. Derivation 2: Analogy with W_D

The expression for W_P may be obtained by modifying the expression for W_D . Exchanging l_i and L_i and their primes in W_D (which incurs phase factors of $(-1)^{l_i+L_i+L}$ etc., as in the HELIUM analogy), and changing D_N to $E(t)r \cos \theta$, we have that

$$W_{P_{pp'}}(t) = (-1)^{L+L'+1}(-1)^{l_i-M_L+L_i} \sqrt{(2L'+1)(2L+1)} \begin{pmatrix} L & L' & 1 \\ -M_L & M_L & 0 \end{pmatrix} \left\{ \begin{array}{ccc} L & L' & 1 \\ l'_i & l_i & L_i \end{array} \right\} \times \delta_{\alpha_i \alpha'_i} E(t) \langle l_i \| T^1 \| l'_i \rangle \delta_{SS'} \delta_{S_i S'_i} \delta_{M_S M'_S} \delta_{M_{S_i} M'_{S_i}} \delta_{M_L M'_L} \delta_{L_i L'_i}, \quad (89)$$

where the first factor of $(-1)^{L+L'+1}$ arises from switching the order of the residual ion and electronic angular momenta, as in Eq. (57). In this case, the reduced matrix element may be evaluated directly, giving

$$\langle l_i \| T^1 \| l'_i \rangle = (-1)^{l_i} i^{l'_i - l_i} \sqrt{(2l_i + 1)(2l'_i + 1)} \begin{pmatrix} l_i & 1 & l'_i \\ 0 & 0 & 0 \end{pmatrix} r. \quad (90)$$

Therefore,

$$W_{P_{pp'}}(t) = i^{l'_i - l_i} E(t) r (-1)^{L+L'+1-M_L+L_i} \sqrt{(2L'+1)(2L+1)(2l_i+1)(2l'_i+1)} \times \delta_{\alpha_i \alpha'_i} \begin{pmatrix} l_i & 1 & l'_i \\ 0 & 0 & 0 \end{pmatrix} \begin{pmatrix} L & L' & 1 \\ -M_L & M_L & 0 \end{pmatrix} \left\{ \begin{array}{ccc} L & L' & 1 \\ l'_i & l_i & L_i \end{array} \right\} \times \delta_{SS'} \delta_{S_i S'_i} \delta_{M_S M'_S} \delta_{M_{S_i} M'_{S_i}} \delta_{M_L M'_L} \delta_{L_i L'_i}, \quad (91)$$

which agrees with the result of Derivation 1 given in Eq. (59).

C.5. Derivation 3: Reduced matrix elements

Starting from Eq. (5.64) in Zare's book [2],

$$\langle \alpha_i L_i l_i LM_L | r_0^{(1)} | \alpha'_i L'_i l'_i L' M'_L \rangle = (-1)^{L-M_L} \begin{pmatrix} L & 1 & L' \\ -M_L & 0 & M'_L \end{pmatrix} \langle \alpha_i L_i l_i L \| r^{(1)} \| \alpha'_i L'_i l'_i L' \rangle. \quad (92)$$

Now noting the order of the angular momenta, I use Eq. (5.73) of [2] (NOT Eq. (5.72)) to get

$$\langle \alpha_i L_i l_i LM_L | r_0^{(1)} | \alpha'_i L'_i l'_i L' M'_L \rangle = (-1)^{L-M_L} \begin{pmatrix} L & 1 & L' \\ -M_L & 0 & M'_L \end{pmatrix} \times \delta_{\alpha_i \alpha'_i} \delta_{L_i L'_i} (-1)^{L_i+l'_i+L+1} \sqrt{[L'][L]} \left\{ \begin{array}{ccc} l_i & L & L_i \\ L' & l_i & 1 \end{array} \right\} \langle l_i \| r^{(1)} \| l'_i \rangle. \quad (93)$$

Evaluating the reduced matrix element then gives

$$\begin{aligned} \langle \alpha_i L_i l_i LM_L | r_0^{(1)} | \alpha'_i L'_i l'_i L' M'_L \rangle &= (-1)^{L-M_L} \begin{pmatrix} L & 1 & L' \\ -M_L & 0 & M_L \end{pmatrix} \\ &\times \delta_{\alpha_i \alpha'_i} \delta_{L_i L'_i} \delta_{M_L M'_L} (-1)^{L_i + l'_i + L+1} \sqrt{[L'][L]} \left\{ \begin{array}{ccc} l_i & L & L_i \\ L' & l_i & 1 \end{array} \right\} \\ &\times i^{l'_i + 1 - l_i} (-1)^{l_i} \sqrt{[l'_i][l_i]} \begin{pmatrix} l_i & 1 & l'_i \\ 0 & 0 & 0 \end{pmatrix} r. \end{aligned} \quad (94)$$

The phase factor is now $(-1)^{L-M_L+L_i+l'_i+L+1+l_i} = (-1)^{-M_L+L_i}$ since $l'_i + 1 + l_i$ is even. Now rearranging the columns (uneven permutation of columns 2 and 3, giving factor of $(-1)^{L+L'+1}$) of the M_L -dependent 3-j symbol, I find that

$$\begin{aligned} \langle \alpha_i L_i l_i LM_L | r_0^{(1)} | \alpha'_i L'_i l'_i L' M'_L \rangle &= i^{l'_i + 1 - l_i} (-1)^{L+L'+1+L_i-M_L} \delta_{\alpha_i \alpha'_i} \delta_{L_i L'_i} \delta_{M_L M'_L} \sqrt{[L'][L][l'_i][l_i]} \\ &\times \begin{pmatrix} l_i & 1 & l'_i \\ 0 & 0 & 0 \end{pmatrix} \begin{pmatrix} L & L' & 1 \\ -M_L & M_L & 0 \end{pmatrix} \left\{ \begin{array}{ccc} L & L' & 1 \\ l'_i & l_i & L_i \end{array} \right\} r. \end{aligned} \quad (95)$$

Now

$$W_{P_{pp'}} = -iE(t) \langle \alpha_i L_i l_i LM_L | r_0^{(1)} | \alpha'_i L'_i l'_i L' M'_L \rangle \delta_{SS'} \delta_{S_i S'_i} \delta_{M_S M'_S} \delta_{M_{S_i} M'_{S_i}} \quad (96)$$

so

$$\begin{aligned} W_{P_{pp'}} &= i^{l'_i - l_i} E(t) r (-1)^{L+L'+1+L_i-M_L} \delta_{\alpha_i \alpha'_i} \delta_{L_i L'_i} \delta_{M_L M'_L} \sqrt{[L'][L][l'_i][l_i]} \\ &\times \begin{pmatrix} l_i & 1 & l'_i \\ 0 & 0 & 0 \end{pmatrix} \begin{pmatrix} L & L' & 1 \\ -M_L & M_L & 0 \end{pmatrix} \left\{ \begin{array}{ccc} L & L' & 1 \\ l'_i & l_i & L_i \end{array} \right\} \\ &\times \delta_{SS'} \delta_{S_i S'_i} \delta_{M_S M'_S} \delta_{M_{S_i} M'_{S_i}}, \end{aligned} \quad (97)$$

which agrees with Eq. (59) and (91).

VII. Other polarizations

For other polarizations, we require the angular matrix elements involving x and y . For mixed $x - y$ plane polarization, we have that

$$x \pm iy = r \sin \theta e^{\pm i\phi} = \mp r \sqrt{\frac{8\pi}{3}} Y_{1\pm 1}(\theta, \phi), \quad (98)$$

so, noting the extra factor of $\sqrt{2}$, we have

$$\begin{aligned} \langle \alpha_i L_i l_i LM_L | \sin \theta e^{\pm i\phi} | \alpha'_i L'_i l'_i L' M'_L \rangle &= \mp i^{l'_i - l_i} (-1)^{L+L'+1+L_i-M_L} \sqrt{2(2L+1)(2L'+1)(2l_i+1)(2l'_i+1)} \\ &\times \delta_{\alpha_i \alpha'_i} \delta_{L_i L'_i} \delta_{M'_L, M_L \mp 1} \left(\begin{array}{ccc} l_i & 1 & l'_i \\ 0 & 0 & 0 \end{array} \right) \left\{ \begin{array}{ccc} L & L' & 1 \\ l'_i & l_i & L_i \end{array} \right\} \left(\begin{array}{ccc} L & L' & 1 \\ -M_L & M'_L & \pm 1 \end{array} \right). \end{aligned} \quad (99)$$

Now given that

$$x = \frac{1}{2} r \sin \theta (e^{i\phi} + e^{-i\phi}), \quad (100)$$

$$y = i \frac{1}{2} r \sin \theta (e^{-i\phi} - e^{i\phi}), \quad (101)$$

then the result for x -axis linear polarization is (see also Eq. (C.8) in [3])

$$\begin{aligned} \langle \alpha_i L_i l_i LM_L | \sin \theta \cos \phi | \alpha'_i L'_i l'_i L' M'_L \rangle &= i^{l'_i - l_i} (-1)^{L+L'+1+L_i-M_L} \sqrt{\frac{(2L+1)(2L'+1)(2l_i+1)(2l'_i+1)}{2}} \\ &\times \delta_{\alpha_i \alpha'_i} \delta_{L_i, L'_i} \left(\begin{array}{ccc} l_i & 1 & l'_i \\ 0 & 0 & 0 \end{array} \right) \left\{ \begin{array}{ccc} L & L' & 1 \\ l'_i & l_i & L_i \end{array} \right\} \\ &\times \left[\delta_{M'_L, M_L+1} \left(\begin{array}{ccc} L & L' & 1 \\ -M_L & M'_L & -1 \end{array} \right) - \delta_{M'_L, M_L-1} \left(\begin{array}{ccc} L & L' & 1 \\ -M_L & M'_L & 1 \end{array} \right) \right]. \end{aligned} \quad (102)$$

and for y -axis polarization we have

$$\begin{aligned} \langle \alpha_i L_i l_i LM_L | \sin \theta \sin \phi | \alpha'_i L'_i l'_i L' M'_L \rangle &= i^{l'_i - l_i + 1} (-1)^{L+L'+1+L_i-M_L} \sqrt{\frac{(2L+1)(2L'+1)(2l_i+1)(2l'_i+1)}{2}} \\ &\times \delta_{\alpha_i \alpha'_i} \delta_{L_i, L'_i} \left(\begin{array}{ccc} l_i & 1 & l'_i \\ 0 & 0 & 0 \end{array} \right) \left\{ \begin{array}{ccc} L & L' & 1 \\ l'_i & l_i & L_i \end{array} \right\} \\ &\times \left[\delta_{M'_L, M_L+1} \left(\begin{array}{ccc} L & L' & 1 \\ -M_L & M'_L & -1 \end{array} \right) + \delta_{M'_L, M_L-1} \left(\begin{array}{ccc} L & L' & 1 \\ -M_L & M'_L & 1 \end{array} \right) \right]. \end{aligned} \quad (103)$$

A. Daniel expressions

Daniel derives an expression for $\mathbf{E}(t) \cdot \mathbf{r}$ in spherical components, which may be used to derive matrix elements involving $r_0, \pm 1$, rather than x, y, z . His expressions for $\mu = 0, \pm 1$ are

$$\begin{aligned} \langle \alpha_i L_i l_i LM_L | r_\mu^{(1)} | \alpha'_i L'_i l'_i L' M'_L \rangle &= (-1)^{L+L'} \sqrt{(2l'_i + 1)(2L + 1)} (LM_L 1(-\mu) | L' M'_L) \\ &\times \frac{a(l'_i)}{(l_i 0 1 0 | l'_i 0)} W(1l'_i LL_i, l_i L') r \delta_{\alpha_i \alpha'_i} \delta_{L'_i L_i} \delta_{M_L, M'_L + \mu}. \end{aligned} \quad (104)$$

Note from Eq. (200) that $a(l'_i)$ contains a factor -1, which ultimately makes the overall sign term $(-1)^{L+L'+1}$. This provides a generalization of the $\mu = 0$ result given in Eq. (95), which may be extended simply to

$$\begin{aligned} \langle \alpha_i L_i l_i LM_L | r_\mu^{(1)} | \alpha'_i L'_i l'_i L' M'_L \rangle &= i^{l'_i + 1 - l_i} (-1)^{L+L'+1+L_i-M_L} \delta_{\alpha_i \alpha'_i} \delta_{L_i L'_i} \delta_{M_L, M'_L + \mu} \sqrt{[L'][L][l'_i][l_i]} \\ &\times \begin{pmatrix} l_i & 1 & l'_i \\ 0 & 0 & 0 \end{pmatrix} \begin{pmatrix} L & L' & 1 \\ -M_L & M'_L & \mu \end{pmatrix} \left\{ \begin{array}{ccc} L & L' & 1 \\ l'_i & l_i & L_i \end{array} \right\} r. \end{aligned} \quad (105)$$

Now since

$$\mathbf{E}(t) \cdot \mathbf{r} = E_x x + E_y y + E_z z = \sum_{\mu=0,\pm 1} (-1)^\mu E_\mu r_{-\mu} = E_0 r_0 - E_{-1} r_1 - E_1 r_{-1}, \quad (106)$$

and

$$E_1 = -i \frac{1}{\sqrt{2}} (E_x + i E_y), \quad (107)$$

$$E_0 = i E_z, \quad (108)$$

$$E_{-1} = i \frac{1}{\sqrt{2}} (E_x - i E_y), \quad (109)$$

then (CHECK!!)

$$x = -i \frac{1}{\sqrt{2}} (r_{-1}^{(1)} - r_1^{(1)}), \quad (110)$$

$$y = \frac{1}{\sqrt{2}} (r_{-1}^{(1)} + r_1^{(1)}), \quad (111)$$

$$z = -i r_0. \quad (112)$$

Therefore, we may construct the x and y matrix elements from Daniel's expressions, and compare with those given previously. We have that

$$\langle \alpha_i L_i l_i LM_L | x | \alpha'_i L'_i l'_i L' M'_L \rangle = -i \frac{1}{\sqrt{2}} \langle \alpha_i L_i l_i LM_L | r_{-1}^{(1)} - r_1^{(1)} | \alpha'_i L'_i l'_i L' M'_L \rangle \quad (113)$$

which by Eq. (105) is

$$\begin{aligned} \langle \alpha_i L_i l_i LM_L | r \sin \theta \cos \phi | \alpha'_i L'_i l'_i L' M'_L \rangle &= i^{l'_i - l_i} (-1)^{L+L'+1+L_i-M_L} \delta_{\alpha_i \alpha'_i} \delta_{L_i L'_i} \\ &\quad \times \sqrt{\frac{[L'][L][l'_i][l_i]}{2}} \begin{pmatrix} l_i & 1 & l'_i \\ 0 & 0 & 0 \end{pmatrix} \\ &\quad \times \left[\delta_{M_L, M'_L - 1} \begin{pmatrix} L & L' & 1 \\ -M_L & M'_L & -1 \end{pmatrix} - \delta_{M_L, M'_L + 1} \begin{pmatrix} L & L' & 1 \\ -M_L & M'_L & 1 \end{pmatrix} \right] \left\{ \begin{array}{ccc} L & L' & 1 \\ l'_i & l_i & L_i \end{array} \right\} r, \end{aligned} \quad (114)$$

which confirms Eq. (102).

Now the y matrix element may be given as

$$\begin{aligned} \langle \alpha_i L_i l_i LM_L | r \sin \theta \sin \phi | \alpha'_i L'_i l'_i L' M'_L \rangle &= i^{l'_i + 1 - l_i} (-1)^{L+L'+1+L_i-M_L} \delta_{\alpha_i \alpha'_i} \delta_{L_i L'_i} \\ &\quad \times \sqrt{\frac{[L'][L][l'_i][l_i]}{2}} \begin{pmatrix} l_i & 1 & l'_i \\ 0 & 0 & 0 \end{pmatrix} \\ &\quad \times \left[\delta_{M_L, M'_L - 1} \begin{pmatrix} L & L' & 1 \\ -M_L & M'_L & -1 \end{pmatrix} + \delta_{M_L, M'_L + 1} \begin{pmatrix} L & L' & 1 \\ -M_L & M'_L & 1 \end{pmatrix} \right] \left\{ \begin{array}{ccc} L & L' & 1 \\ l'_i & l_i & L_i \end{array} \right\} r, \end{aligned} \quad (115)$$

which confirms Eq. (103).

VIII. Summary of length-gauge W_P matrix elements for different polarizations

A. Spherical components

In the previous sections it was established that (see Eq. (104))

$$\begin{aligned} \langle \alpha_i L_i l_i LM_L | r_\mu^{(1)} | \alpha'_i L'_i l'_i L' M'_L \rangle &= (-1)^{L+L'} \sqrt{(2l'_i + 1)(2L + 1)} (LM_L 1(-\mu) | L' M'_L) \\ &\quad \times \frac{a(l'_i)}{(l_i 0 1 0 | l'_i 0)} W(1l'_i LL_i, l_i L') r \delta_{\alpha_i \alpha'_i} \delta_{L'_i L_i} \delta_{M_L, M'_L + \mu}. \end{aligned} \quad (116)$$

Therefore, the W_P interaction Hamiltonian has three terms, $\mu = -1, 0, 1$, where

$$\begin{aligned} W_{P_{pp'}}^{(\mu)} &= E_\mu(t) \langle \alpha_i L_i l_i LM_L | r_\mu^{(1)} | \alpha'_i L'_i l'_i L' M'_L \rangle \\ &\quad \times \delta_{SS'} \delta_{S_i S'_i} \delta_{M_S M'_S} \delta_{M_{S_i} M'_{S_i}}, \end{aligned} \quad (117)$$

where the -1,0,1 components are

$$\begin{aligned}
 W_{P_{pp'}}^{(-1)} = & E_{-1}(t)(-1)^{L+L'} \sqrt{(2l'_i + 1)(2L + 1)} (LM_L 1 + 1 | L' M'_L) \delta_{M_L, M'_L - 1} \\
 & \times \frac{a(l'_i)}{(l_i 010 | l'_i 0)} W(1l'_i LL_i, l_i L') r \delta_{\alpha_i \alpha'_i} \delta_{L'_i L_i} \\
 & \times \delta_{SS'} \delta_{S_i S'_i} \delta_{M_S M'_S} \delta_{M_{S_i} M'_{S_i}}, \tag{118}
 \end{aligned}$$

$$\begin{aligned}
 W_{P_{pp'}}^{(0)} = & E_0(t)(-1)^{L+L'} \sqrt{(2l'_i + 1)(2L + 1)} (LM_L 10 | L' M'_L) \delta_{M_L, M'_L} \\
 & \times \frac{a(l'_i)}{(l_i 010 | l'_i 0)} W(1l'_i LL_i, l_i L') r \delta_{\alpha_i \alpha'_i} \delta_{L'_i L_i} \\
 & \times \delta_{SS'} \delta_{S_i S'_i} \delta_{M_S M'_S} \delta_{M_{S_i} M'_{S_i}}, \tag{119}
 \end{aligned}$$

$$\begin{aligned}
 W_{P_{pp'}}^{(1)} = & E_1(t)(-1)^{L+L'} \sqrt{(2l'_i + 1)(2L + 1)} (LM_L 1 - 1 | L' M'_L) \delta_{M_L, M'_L + 1} \\
 & \times \frac{a(l'_i)}{(l_i 010 | l'_i 0)} W(1l'_i LL_i, l_i L') r \delta_{\alpha_i \alpha'_i} \delta_{L'_i L_i} \\
 & \times \delta_{SS'} \delta_{S_i S'_i} \delta_{M_S M'_S} \delta_{M_{S_i} M'_{S_i}}. \tag{120}
 \end{aligned}$$

B. Cartesian components (CHECK!!!!)

Using

$$x = -i \frac{1}{\sqrt{2}} (r_{-1}^{(1)} - r_1^{(1)}), \tag{121}$$

$$y = \frac{1}{\sqrt{2}} (r_{-1}^{(1)} + r_1^{(1)}), \tag{122}$$

$$z = -ir_0. \tag{123}$$

for x -axis polarization we have (NOT CORRECT, CHECK E-FIELD FACTORS!!)

$$\begin{aligned}
 W_{P_{pp'}}^{(x)} = & -i E_x(t)(-1)^{L+L'} \sqrt{\frac{(2l'_i + 1)(2L + 1)}{2}} \frac{a(l'_i)}{(l_i 010 | l'_i 0)} W(1l'_i LL_i, l_i L') r \delta_{\alpha_i \alpha'_i} \delta_{L'_i L_i} \\
 & \times [(LM_L 11 | L' M'_L) \delta_{M_L, M'_L - 1} - (LM_L 1 - 1 | L' M'_L) \delta_{M_L, M'_L + 1}], \tag{124}
 \end{aligned}$$

for y -axis polarization we have

$$\begin{aligned}
 W_{P_{pp'}}^{(y)} = & E_y(t)(-1)^{L+L'} \sqrt{\frac{(2l'_i + 1)(2L + 1)}{2}} \frac{a(l'_i)}{(l_i 010 | l'_i 0)} W(1l'_i LL_i, l_i L') r \delta_{\alpha_i \alpha'_i} \delta_{L'_i L_i} \\
 & \times [(LM_L 11 | L' M'_L) \delta_{M_L, M'_L - 1} + (LM_L 1 - 1 | L' M'_L) \delta_{M_L, M'_L + 1}], \tag{125}
 \end{aligned}$$

for z -axis polarization we have

$$W_{P_{pp'}}^{(z)} = -iE_z(t)(-1)^{L+L'}\sqrt{(2l'_i+1)(2L+1)} \frac{a(l'_i)}{(l_i010|l'_i0)} W(1l'_iLL_i, l_iL')r\delta_{\alpha_i\alpha'_i}\delta_{L'_iL_i} \times (LM_L 10|L'M'_L)\delta_{M_L, M'_L}. \quad (126)$$

IX. Velocity gauge

The velocity-gauge expression for the HELIUM matrix elements are given in [3]. These may be simply generalized to our case. For polarization along the z axis, the velocity gauge $W_{P_{pp'}} f_{p'}$ matrix-vector product becomes

$$W_{P_{pp'}} f_{p'}(r, t) = r \langle \alpha_i L_i l_i LM_L | \left(-\frac{i}{c} A(t) \frac{\partial}{\partial z} \right) \frac{1}{r} f_{p'}(r, t) | \alpha'_i L'_i l'_i L' M'_L \rangle \times \delta_{SS'} \delta_{S_i S'_i} \delta_{M_S M'_S} \delta_{M_{S_i} M'_{S_i}}. \quad (127)$$

Now using the gradient commutator relation from [3],

$$\nabla = \frac{1}{2} [\nabla^2, \mathbf{r}], \quad (128)$$

we have that

$$\frac{\partial}{\partial z} = \frac{1}{2} [\nabla^2, r \cos \theta]. \quad (129)$$

Then I find that (see Appendix D., Eq. (210)),

$$\begin{aligned} & \frac{1}{2} [\nabla^2, r \cos \theta] \frac{1}{r} f_{p'}(r, t) | \alpha'_i L'_i l'_i L' M'_L \rangle \\ &= \left[\frac{\cos \theta}{r} \frac{\partial}{\partial r} + \frac{1}{2r} \left(r \cos \theta \frac{\mathbf{l}^2}{r^2} - \frac{\mathbf{l}^2}{r^2} r \cos \theta \right) \right] f_{p'}(r, t) | \alpha'_i L'_i l'_i L' M'_L \rangle, \\ &= \left[\frac{\cos \theta}{r} \frac{\partial}{\partial r} + \left(\cos \theta \frac{\mathbf{l}^2}{2r^2} - \frac{\mathbf{l}^2}{2r^2} \cos \theta \right) \right] f_{p'}(r, t) | \alpha'_i L'_i l'_i L' M'_L \rangle. \end{aligned} \quad (130)$$

So,

$$\begin{aligned} W_{P_{pp'}} f_{p'}(r, t) &= -\frac{i}{c} A(t) r \left[\frac{1}{r} \frac{\partial}{\partial r} + \frac{l'_i(l'_i+1)}{2r^2} - \frac{l_i(l_i+1)}{2r^2} \right] f_{p'}(r, t) \\ &\quad \times \langle \alpha_i L_i l_i LM_L | \cos \theta | \alpha'_i L'_i l'_i L' M'_L \rangle \\ &\quad \times \delta_{SS'} \delta_{S_i S'_i} \delta_{M_S M'_S} \delta_{M_{S_i} M'_{S_i}}. \end{aligned} \quad (131)$$

Remembering to multiply in the r factor (to cancel $1/r$ on the LHS time derivative), the result is

$$\begin{aligned} W_{P_{pp'}} f_{p'}(r, t) &= -\frac{i}{c} A(t) \left[\frac{\partial}{\partial r} + \frac{l'_i(l'_i+1) - l_i(l_i+1)}{2r} \right] f_{p'}(r, t) \\ &\quad \times \langle \alpha_i L_i l_i LM_L | \cos \theta | \alpha'_i L'_i l'_i L' M'_L \rangle \\ &\quad \times \delta_{SS'} \delta_{S_i S'_i} \delta_{M_S M'_S} \delta_{M_{S_i} M'_{S_i}}. \end{aligned} \quad (132)$$

Therefore, using Eq. (58), the velocity-gauge expression for W_P should be

$$\boxed{W_{P_{pp'}}(t) = -\frac{i}{c}A(t) \left[\frac{\partial}{\partial r} + \frac{l'_i(l'_i+1) - l_i(l_i+1)}{2r} \right] \delta_{SS'} \delta_{S_i S'_i} \delta_{M_S M'_S} \delta_{M_{S_i} M'_{S_i}} \\ \times i^{l'_i - l_i} (-1)^{L+L'+1+L_i-M_L} \sqrt{(2L+1)(2L'+1)(2l_i+1)(2l'_i+1)} \\ \times \delta_{\alpha_i \alpha'_i} \delta_{L_i L'_i} \delta_{M_L M'_L} \begin{Bmatrix} l_i & 1 & l'_i \\ 0 & 0 & 0 \end{Bmatrix} \begin{Bmatrix} L & L' & 1 \\ -M_L & M_L & 0 \end{Bmatrix} \left\{ \begin{array}{ccc} L & L' & 1 \\ l'_i & l_i & L_i \end{array} \right\}. \quad (133)}$$

A. Comparison with other sources

An expression for the velocity-gauge form of W_P was given in Steven Hutchinson's thesis. He gives

$$W_P = -\frac{i}{c}A(t)i^{l'_i - l_i}(-1)^{l_i+L-L_i} \sqrt{(2l_i+1)(2L+1)} \\ \times (l_i 0 1 0 | l'_i 0) (L M_L 1 0 | L' M_L) W(LL_i L' l'_i, l_i 1) \left[\frac{\partial}{\partial r} - \frac{f(l'_i, l_i)}{r} - \frac{1}{r} \right] \\ \times \delta_{SS'} \delta_{S_i S'_i} \delta_{M_S M'_S} \delta_{M_{S_i} M'_{S_i}} \delta_{L_i L'_i} \delta_{M_L M'_L} \delta_{m_i m'_i} \delta_{M_{L_i} M'_{L_i}}. \quad (134)$$

There may be a typo here, since the Racah W coefficient gives the wrong form:

$$W(LL_i L' l'_i, l_i 1) = (-1)^{L+L_i+L+l'_i} \left\{ \begin{array}{ccc} L & L_i & l_i \\ l'_i & L' & 1 \end{array} \right\} = (-1)^{L+L_i+L+l'_i} \left\{ \begin{array}{ccc} L & L' & 1 \\ l'_i & L_i & l_i \end{array} \right\}. \quad (135)$$

The Racah coefficient should be same in both length and velocity gauges. If L_i and l_i were swapped in the W coefficient, this would give the correct 6-j symbol.

If this change is applied, Steven's result becomes identical to Eq. (133). Until the 'error' in Eq. (134) is proved to be a typo, this does not constitute a verification of Eq. (133).

B. Other polarizations

For polarization along the x axis, the velocity gauge $W_{P_{pp'}} f_{p'}$ matrix-vector product becomes

$$W_{P_{pp'}} f_{p'}(r, t) = r \langle \alpha_i L_i l_i L M_L | \left(-\frac{i}{c} A(t) \frac{\partial}{\partial x} \right) \frac{1}{r} f_{p'}(r, t) | \alpha'_i L'_i l'_i L' M'_L \rangle \\ \times \delta_{SS'} \delta_{S_i S'_i} \delta_{M_S M'_S} \delta_{M_{S_i} M'_{S_i}}. \quad (136)$$

Now using the gradient commutator relation

$$\nabla = \frac{1}{2} [\nabla^2, \mathbf{r}], \quad (137)$$

we have that

$$\frac{\partial}{\partial x} = \frac{1}{2} [\nabla^2, r \sin \theta \cos \phi]. \quad (138)$$

Then I find that,

$$\begin{aligned} & \frac{1}{2} [\nabla^2, r \sin \theta \cos \phi] \frac{1}{r} f_{p'}(r, t) |\alpha'_i L'_i l'_i L' M'_L\rangle \\ &= \left[\frac{\sin \theta \cos \phi}{r} \frac{\partial}{\partial r} + \frac{1}{2r} \left(r \sin \theta \cos \phi \frac{l^2}{r^2} - \frac{l^2}{r^2} r \sin \theta \cos \phi \right) \right] f_{p'}(r, t) |\alpha'_i L'_i l'_i L' M'_L\rangle, \\ &= \left[\frac{\sin \theta \cos \phi}{r} \frac{\partial}{\partial r} + \left(\sin \theta \cos \phi \frac{l^2}{2r^2} - \frac{l^2}{2r^2} \sin \theta \cos \phi \right) \right] f_{p'}(r, t) |\alpha'_i L'_i l'_i L' M'_L\rangle. \end{aligned} \quad (139)$$

So,

$$\begin{aligned} W_{P_{pp'}} f_{p'}(r, t) &= -\frac{i}{c} A(t) r \left[\frac{1}{r} \frac{\partial}{\partial r} + \frac{l'_i(l'_i + 1)}{2r^2} - \frac{l_i(l_i + 1)}{2r^2} \right] f_{p'}(r, t) \\ &\quad \times \langle \alpha_i L_i l_i LM_L | \sin \theta \cos \phi | \alpha'_i L'_i l'_i L' M'_L \rangle \\ &\quad \times \delta_{SS'} \delta_{S_i S'_i} \delta_{M_S M'_S} \delta_{M_{S_i} M'_{S_i}}. \end{aligned} \quad (140)$$

Remembering to multiply in the r factor (to cancel $1/r$ on the LHS time derivative), the result is

$$\begin{aligned} W_{P_{pp'}} f_{p'}(r, t) &= -\frac{i}{c} A(t) \left[\frac{\partial}{\partial r} + \frac{l'_i(l'_i + 1) - l_i(l_i + 1)}{2r} \right] f_{p'}(r, t) \\ &\quad \times \langle \alpha_i L_i l_i LM_L | \sin \theta \cos \phi | \alpha'_i L'_i l'_i L' M'_L \rangle \\ &\quad \times \delta_{SS'} \delta_{S_i S'_i} \delta_{M_S M'_S} \delta_{M_{S_i} M'_{S_i}}. \end{aligned} \quad (141)$$

Using the commutator relation to introduce the Laplacian means that no angular derivatives need to be taken, so that angular terms simply pass through the expressions as multiplicative factors. Therefore, extension of this result to other polarizations is trivial.

For y -axis polarization, Eq. (141) becomes

$$\begin{aligned} W_{P_{pp'}} f_{p'}(r, t) &= -\frac{i}{c} A(t) \left[\frac{\partial}{\partial r} + \frac{l'_i(l'_i + 1) - l_i(l_i + 1)}{2r} \right] f_{p'}(r, t) \\ &\quad \times \langle \alpha_i L_i l_i LM_L | \sin \theta \sin \phi | \alpha'_i L'_i l'_i L' M'_L \rangle \\ &\quad \times \delta_{SS'} \delta_{S_i S'_i} \delta_{M_S M'_S} \delta_{M_{S_i} M'_{S_i}}. \end{aligned} \quad (142)$$

These expressions may be recast in terms of $r_{0,\pm 1}^{(1)}$ simply as

$$\begin{aligned} W_{P_{pp'}} f_{p'}(r, t) &= -\frac{i}{c} A(t) \left[\frac{\partial}{\partial r} + \frac{l'_i(l'_i + 1) - l_i(l_i + 1)}{2r} \right] f_{p'}(r, t) \\ &\quad \times \left\langle \alpha_i L_i l_i LM_L \left| \frac{-ir_\mu^{(1)}}{r} \right| \alpha'_i L'_i l'_i L' M'_L \right\rangle \\ &\quad \times \delta_{SS'} \delta_{S_i S'_i} \delta_{M_S M'_S} \delta_{M_{S_i} M'_{S_i}}. \end{aligned} \quad (143)$$

Writing these in terms of Clebsch-Gordan and Racah W coefficients, using Eq. (104), to give

$$\begin{aligned} W_{P_{pp'}} f_{p'}(r, t) &= -\frac{i}{c} A(t) \left[\frac{\partial}{\partial r} + \frac{l'_i(l'_i + 1) - l_i(l_i + 1)}{2r} \right] f_{p'}(r, t) \\ &\times (-1)^{L+L'} \sqrt{(2l'_i + 1)(2L + 1)} (LM_L 1(-\mu) | L'M'_L) \frac{(-i)a(l'_i)}{(l_i 010 | l'_i 0)} W(1l'_i LL_i, l_i L') \\ &\times \delta_{\alpha_i \alpha'_i} \delta_{L'_i L_i} \delta_{M_L, M'_L + \mu} \delta_{SS'} \delta_{S_i S'_i} \delta_{M_S M'_S} \delta_{M_{S_i} M'_{S_i}}, \end{aligned} \quad (144)$$

Now we have that

$$\boxed{\frac{l'_i(l'_i + 1) - l_i(l_i + 1)}{2} = \begin{cases} l'_i & \text{for } l_i = l'_i - 1 \\ -l'_i - 1 & \text{for } l_i = l'_i + 1 \end{cases} = b(l'_i)}, \quad (145)$$

and so the expression for $W_{P_{pp'}}$ itself resembles Burke's original form (note that the minus sign from $-ia(l'_i)$ in Eq. (144) has been added to the overall sign term, giving $(-1)^{L+L'+1}$)

$$\begin{aligned} W_{P_{pp'}} &= -\frac{i}{c} A(t) (-1)^{L+L'+1} \sqrt{(2l'_i + 1)(2L + 1)} ia(l'_i) \frac{(LM_L 1(-\mu) | L'M'_L)}{(l_i 010 | l'_i 0)} W(1l'_i LL_i, l_i L') \\ &\times \left[\frac{\partial}{\partial r} + \frac{b(l'_i)}{r} \right] \delta_{\alpha_i \alpha'_i} \delta_{L'_i L_i} \delta_{M_L, M'_L + \mu} \delta_{SS'} \delta_{S_i S'_i} \delta_{M_S M'_S} \delta_{M_{S_i} M'_{S_i}}. \end{aligned} \quad (146)$$

Now using Eq. (82) for $ia(l'_i)$, we have that

$$\boxed{\begin{aligned} W_{P_{pp'}} &= -\frac{i}{c} A(t) (-1)^{L+L'+1} \sqrt{(2l_i + 1)(2L + 1)} i^{l'_i - l_i} (l_i 010 | l'_i 0) (LM_L 1(-\mu) | L'M'_L) W(1l'_i LL_i, l_i L') \\ &\times \left[\frac{\partial}{\partial r} + \frac{b(l'_i)}{r} \right] \delta_{\alpha_i \alpha'_i} \delta_{L'_i L_i} \delta_{M_L, M'_L + \mu} \delta_{SS'} \delta_{S_i S'_i} \delta_{M_S M'_S} \delta_{M_{S_i} M'_{S_i}}. \end{aligned}} \quad (147)$$

To compare directly with Daniel's expression, the Clebsch-Gordan coefficient needs to be modified. Using

$$(l_i 010 | l'_i 0) = (-1)^{l'_i - l_i} \sqrt{\frac{2l'_i + 1}{2l_i + 1}} (10l'_i 0 | l_i 0) = (-1) \sqrt{\frac{2l'_i + 1}{2l_i + 1}} (10l'_i 0 | l_i 0), \quad (148)$$

I find that

$$W_{P_{pp'}} = -\frac{i}{c} A(t) (-1)^{L+L'} \sqrt{(2l'_i + 1)(2L + 1)} i^{l'_i - l_i} (10l'_i 0 | l_i 0) (LM_L 1(-\mu) | L' M'_L) W(1l'_i LL_i, l_i L') \\ \times \left[\frac{\partial}{\partial r} + \frac{b(l'_i)}{r} \right] \delta_{\alpha_i \alpha'_i} \delta_{L'_i L_i} \delta_{M_L, M'_L + \mu} \delta_{SS'} \delta_{S_i S'_i} \delta_{M_S M'_S} \delta_{M_{S_i} M'_{S_i}}, \quad (149)$$

which agrees with Daniel's expression.

X. Comment on the use of Burke's equation (A2.17)

Equation (A2.17) on page 399 of Burke's book [4] seems to be the source of Eq. (A13) for W_P in the 2009 paper. Burke defines W_P in Eq. (A2.12) in the velocity gauge form of the R -matrix-Floquet formalism as

$$W_P = \langle r_{N+1}^{-1} \bar{\phi}_i^\Gamma | i \frac{A_0}{2c} \hat{\epsilon} \cdot \mathbf{p}_{N+1} | r_{N+1}^{-1} \bar{\phi}_{i'}^{\Gamma'} \rangle (\delta_{nn'+1} - \delta_{nn'-1}). \quad (150)$$

It seems that this expression was used to find $\langle r_{N+1}^{-1} \bar{\phi}_i^\Gamma | \hat{\epsilon} \cdot \mathbf{p}_{N+1} | r_{N+1}^{-1} \bar{\phi}_{i'}^{\Gamma'} \rangle$, from which a length-gauge expression for $\langle r_{N+1}^{-1} \bar{\phi}_i^\Gamma | \hat{\epsilon} \cdot \mathbf{r}_{N+1} | r_{N+1}^{-1} \bar{\phi}_{i'}^{\Gamma'} \rangle$ was derived by analogy. Below, I attempt to go through the details which may have given Eq. (A13) in the 2009 paper.

Since a minus sign appears in front of the $\delta_{nn'-1}$ term, we should focus on the coefficient of $\delta_{nn'+1}$ to obtain an expression for $\langle r_{N+1}^{-1} \bar{\phi}_i^\Gamma | \hat{\epsilon} \cdot \mathbf{p}_{N+1} | r_{N+1}^{-1} \bar{\phi}_{i'}^{\Gamma'} \rangle$. In Burke's Eq. (A2.17), the coefficient of $\delta_{nn'+1}$ is (removing the $iA_0/2c$ prefactor for simplicity)

$$\langle r_{N+1}^{-1} \bar{\phi}_i^\Gamma | \hat{\epsilon} \cdot \mathbf{p}_{N+1} | r_{N+1}^{-1} \bar{\phi}_{i'}^{\Gamma'} \rangle = -(-1)^{L+L'} \sqrt{(2l'_i + 1)(2L + 1)} \frac{(LM_L 10 | L' M_L)}{(l_i 010 | l'_i 0)} W(1l'_i LL_i, l_i L') \\ \times \left(\frac{d}{dr} + \frac{b(l'_i)}{r} \right) \delta_{SS'} \delta_{M_S M'_{S'}} \delta_{S_i S'_i} \delta_{M_{S_i} M'_{S_i}} \delta_{L_i L'_i} \delta_{M_{L_i} M'_{L_i}} \delta_{\gamma_i \gamma'_i}. \quad (151)$$

The minus sign appearing before the $(-1)^{L+L'}$ term could easily be overlooked — the sign within the $(\delta_{nn'+1} - \delta_{nn'-1})$ term in Burke's Floquet expression changes between Eq. (A2.12) and (A2.17).

Now, the only gauge-dependent aspect of this expression is the coupling term, which in velocity gauge is

$$\langle Y_{l_i 0} | \hat{\epsilon} \cdot \mathbf{p} | Y_{l'_i 0} \rangle = \begin{cases} -\frac{l'_i + 1}{\sqrt{(2l'_i + 1)(2l'_i + 3)}} \left(\frac{d}{dr} - \frac{l'_i}{r} \right) & \text{for } l_i = l'_i + 1 \\ \frac{l'}{\sqrt{(2l'_i - 1)(2l'_i + 1)}} \left(\frac{d}{dr} + \frac{l'_i + 1}{r} \right) & \text{for } l_i = l'_i - 1 \end{cases} \quad (152)$$

Now since (notation issue here — multiplying factor of r from the LHS!)

$$r \frac{d}{dr} \left(\frac{f_{p'}(r, t)}{r} \right) = \left(\frac{d}{dr} - \frac{1}{r} \right) f_{p'}(r, t), \quad (153)$$

then

$$\langle Y_{l_i 0} | \hat{\epsilon} \cdot \mathbf{p} | Y'_{l'_i 0} \rangle \frac{f_{p'}(r, t)}{r} = a(l'_i) \left(\frac{d}{dr} + \frac{b(l'_i)}{r} \right) f_{p'}(r, t). \quad (154)$$

Now, from the 2009 paper, we have that in length gauge

$$\langle Y_{l_i 0} | \hat{\epsilon} \cdot \mathbf{r} | Y'_{l'_i 0} \rangle = i a(l'_i) r. \quad (155)$$

A velocity-to-length modification of Burke's expression can be made using the substitutions

$$\mathbf{p} \rightarrow \mathbf{r}, \quad \left(\frac{d}{dr} + \frac{b(l'_i)}{r} \right) \rightarrow ir. \quad (156)$$

Therefore, the length-gauge expression should be Eq. (151) modified according to the substitution in Eq. (156), which would be

$$\begin{aligned} E_0 \langle r_{N+1}^{-1} \bar{\phi}_i^\Gamma | \hat{\epsilon} \cdot \mathbf{r}_{N+1} | r_{N+1}^{-1} \bar{\phi}_{i'}^{\Gamma'} \rangle &= -i E_0 r (-1)^{L+L'} \sqrt{(2l'_i + 1)(2L + 1)} \frac{(LM_L 10 | L' M_L)}{(l_i 010 | l'_i 0)} W(1l'_i LL_i, l_i L') \\ &\times \delta_{SS'} \delta_{M_S M_{S'}} \delta_{S_i S'_i} \delta_{M_{S_i} M'_{S_i}} \delta_{L_i L'_i} \delta_{M_{L_i} M'_{L_i}} \delta_{\gamma_i \gamma'_i}. \end{aligned} \quad (157)$$

This differs from Eq. (A13) in the 2009 paper by a factor of -1. The prefactor of -1 follows from the sign change in Burke's Eq. (A2.17) compared to (A2.12). It appears to be missing in Eq. (A13) of the 2009 paper.

XI. Time propagation

The Taylor series for the coefficients \mathbf{C} satisfying Eq. (7) is

$$\mathbf{C}(t + \delta t) = \sum_{j=0}^{\infty} (\delta t)^j \sum_{k=0}^{\infty} \frac{(-i \delta t \mathbf{H}_I)^k}{(j+k)!} \mathbf{U}_j(t), \quad (158)$$

where

$$\mathbf{U}_0(t) = \mathbf{C}(t), \quad \mathbf{U}_j(t) = \frac{d^{j-1}}{dt^{j-1}} \mathbf{S}(t). \quad (159)$$

The Taylor series can be written as

$$\mathbf{C}(t + \delta t) = \exp(-i \delta t \mathbf{H}_I) \mathbf{C}(t) + \sum_{j=1}^{\infty} (\delta t)^j \phi_j(-i \delta t \mathbf{H}_I) \mathbf{U}_j(t). \quad (160)$$

The ϕ_j function are given by

$$\phi_j(z) = \frac{1}{(j-1)!} \int_0^1 e^{(1-\theta)z} \theta^{j-1} d\theta, \quad j \geq 1. \quad (161)$$

The first few such functions are given by

$$\phi_1(z) = \frac{e^z - 1}{z}, \quad (162)$$

$$\phi_2(z) = \frac{e^z - 1 - z}{z^2}, \quad (163)$$

$$\phi_3(z) = \frac{e^z - 1 - z - \frac{1}{2}z^2}{z^3}. \quad (164)$$

These functions also satisfy the recursion relation

$$\phi_{j+1}(z) = \frac{\phi_j(z) - 1/j!}{z}, \quad \phi_0(z) = e^z, \quad (165)$$

and have the Taylor expansion

$$\phi_j(z) = \sum_{k=0}^{\infty} \frac{z^k}{(j+k)!}. \quad (166)$$

XII. Test case 1: Argon

Test case using a 12-cycle, 2×10^{13} W/cm² pulse with sin² profile, and photon energy $\hbar\omega = 0.33$ a.u., with 3 cycles ramp-on and ramp-off. Using $L \in [0, 2]$ gave 17 LM_L blocks (1 for $^1S^e$, 3 each for $^1P^o$ and $^1P^e$, and 5 each for $^1D^o$ and $^1D^e$). Two residual ion thresholds were included, namely those for $^2S^e$ and $^2P^o$, which gave a total of 34 channels as shown in Table 1. Calculations were run on Aegis10 using 64 cores — 17 for the inner region, as required, and 47 for the outer region. Using `X_Last_Master` = 100 and `X_Last_Others` = 188, and $\delta r = 0.08$ gave an outer region extent of 699.84 a.u..

Results for linear polarization can be found in `/Daniel - codes/linear/ga_linear/Ar_test/`, and for circular polarization in `/Daniel - codes/circular/ga_circ/Ar_test/`. Testing using linear polarization in the x , y and z direction, good agreement found, as shown in Fig. 1.

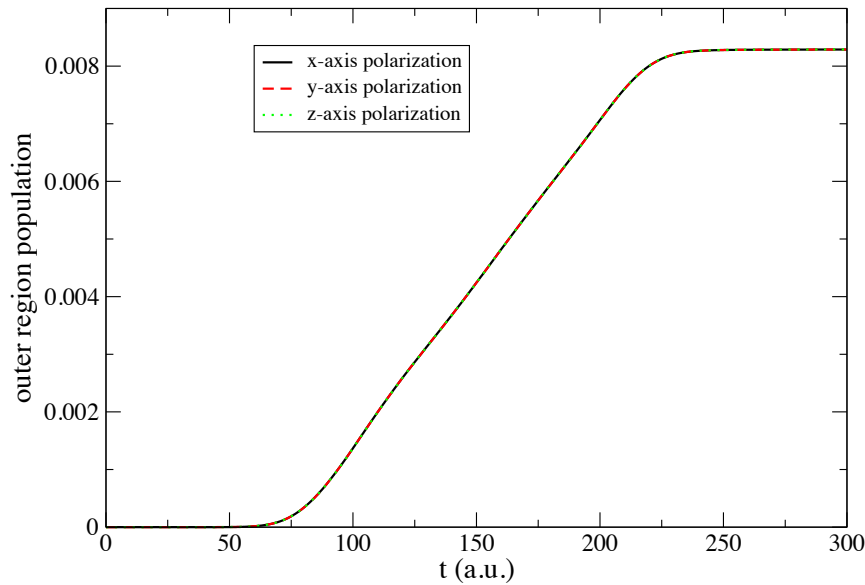


Figure 1: Population in the outer region ($r > 20$ a.u.) for different choice of polarization axis.

Testing using circular polarization of helicity ± 1 , good agreement found — 6-7 significant digits agreement in outer region populations. Outer region population over time shown in Fig. 2.

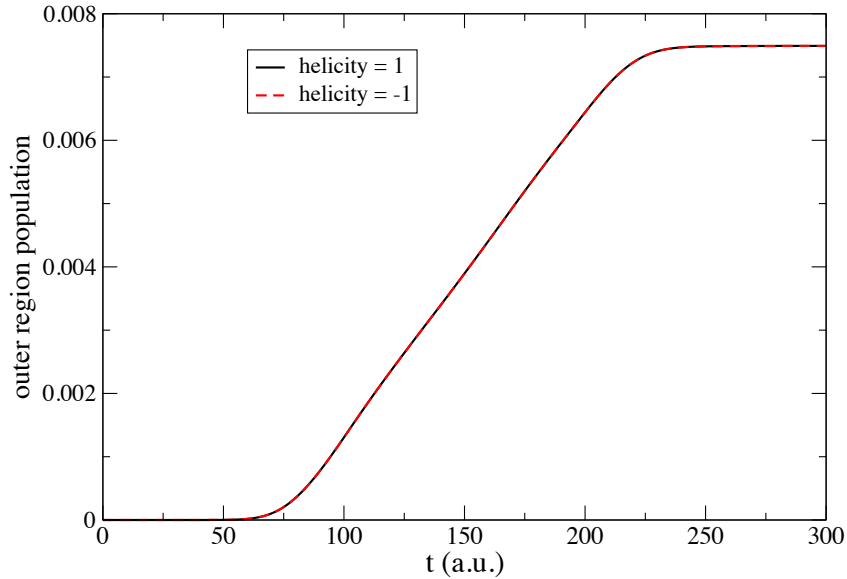


Figure 2: Population in the outer region ($r > 20$ a.u.) for different helicities.

A. Basic tests: Channel populations

Several special test cases can be performed to test the codes. These are:

- **For linear polarization, $\langle M_L \rangle = 0$**

Trivial for z -axis polarization, but for other polarizations it dictates that the distribution of population among sublevels must be symmetric about $M_L = 0$. Therefore sublevels with the same absolute value of M_L are equally populated.

- **For linear polarization, magnetic sublevel branching ratios can be deduced**

For high L values, multiple sublevels will be populated. By considering the pathways to each sublevel, and the relevant M_L -dependent Clebsch-Gordan coefficient in W_P or W_D , branching ratios for, say, the $M_L = 0, 2$ sublevels of ${}^1D^e$ can be calculated. The calculated branching ratios will also be time-independent (and gauge-invariant), so that they must hold at every timestep of a time-dependent calculation.

- **For linear polarization, total ionization yield is frame-independent**

For an electric field of the form $\mathbf{E}(t) = E_0(t) \cos \omega t [\hat{\mathbf{x}} + \epsilon \hat{\mathbf{y}}]$ or $\mathbf{E}(t) = E_0(t) \cos \omega t [\hat{\mathbf{x}} + \epsilon \hat{\mathbf{z}}]$, total yields are independent of ϵ .

- **For $\mathbf{E}(t) = E_0(t) \cos \omega t [\hat{\mathbf{x}} + \epsilon \hat{\mathbf{y}}]$, channel populations are ϵ -independent**

Both total yields and channel yields (and hence, also the magnetic sublevel branching ratios) are independent of ϵ , since the two fields contribute similar dipole selection rules.

- **For $\mathbf{E}(t) = E_0(t) \cos \omega t [\hat{\mathbf{x}} + \epsilon \hat{\mathbf{z}}]$, channel populations are ϵ -dependent**
 Channel yields (and hence, also the magnetic sublevel branching ratios) vary with ϵ since the two fields enforce different dipole selection rules.
- **For circular polarization, $\langle M_L \rangle = \eta M$ ($\eta = \pm 1$ is helicity)**
 If positive helicity favors positive M_L sublevels, then negative helicity favors negative M_L sublevels to the same extent. Linear polarization, $\eta = 0$, could be considered a special case of this relation.
- **For circular polarization, population in $M_L = 0$ is independent of helicity**
 This follows from the property above.

A.1. Linear polarization in the $(x - y)$ plane

Check if $\langle M_L \rangle = 0$ for x -axis polarization

To test the code, I examine the population in certain magnetic sublevels for the Ar test case. For linear polarization, along x , y or $x \pm iy$ directions, channels $\alpha_i L_i l_i LM_L$ and $\alpha_i L_i l_i L(-M_L)$ should be equally populated at all times. Stated another way, the distribution of population among magnetic sublevels should be symmetric about $M_L = 0$. This preserves the obvious $\langle M_L \rangle = 0$ relation for z -axis polarization.

Mathematically, this is because the M_L -dependence W_D and W_P is contained within a Clebsch-Gordan coefficient of the form $(LM_L 1(-\mu) | L'M'_L)$. Consider the $^1S^e \rightarrow ^1P^o$ transition, and the population of the $M_L = \pm 1$ sublevels of $^1P^o$. Population of the $M = 1$ state will be mediated by the Clebsch-Gordan coefficient $(001-1|11)$, and population of the $M = -1$ state will be mediated by the Clebsch-Gordan coefficient $(0011|1-1)$. These coefficients are equal, and so a field polarized along x or y axes will populate the $^1P_{M_L=-1}^o$ and $^1P_{M_L=+1}^o$ states equally at all times (for common values of L_i and l_i).

Physically, this can be thought of in terms of frame rotations. Rotating from z to x involves the J_x operator, which contains equal contributions from J_+ and J_- — so does J_y . However, a general rotation to the $x - y$ plane may not have this property, and so circular polarization will yield $\langle M_L \rangle \neq 0$.

This property is observed in calculations for Ar, as shown in Fig. 3 for the $M_L = \pm 1$ with $L = 1$, and in Fig. 4 for the $M_L = \pm 2$ with $L = 2$.

Branching ratios

Branching ratios for magnetic sublevels may be calculated by considering the lowest-order

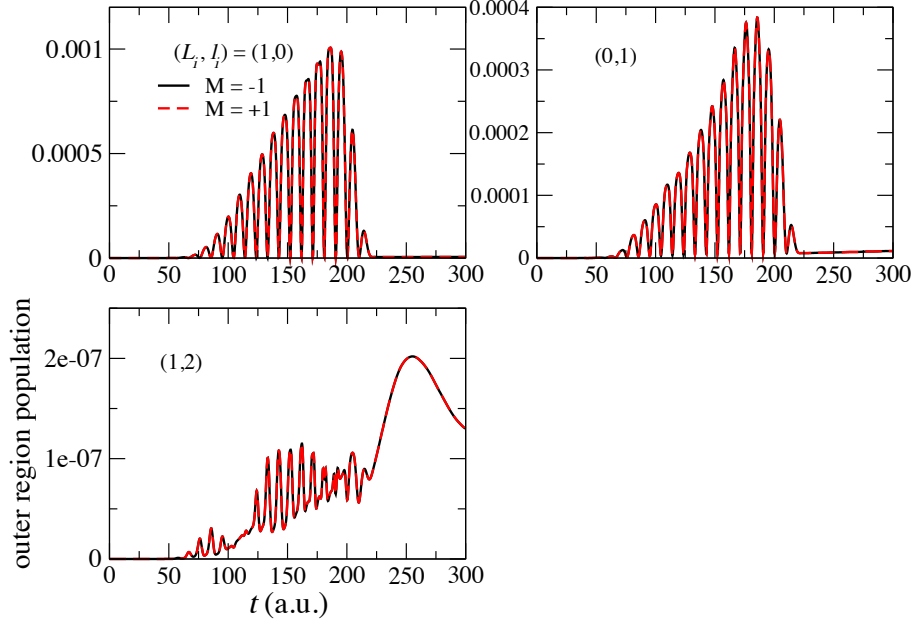


Figure 3: Population in the outer region ($r > 20$ a.u.) for different ${}^1P^o$ channels, for x -axis linear polarization. The values of L_i and l_i are indicated in parentheses.

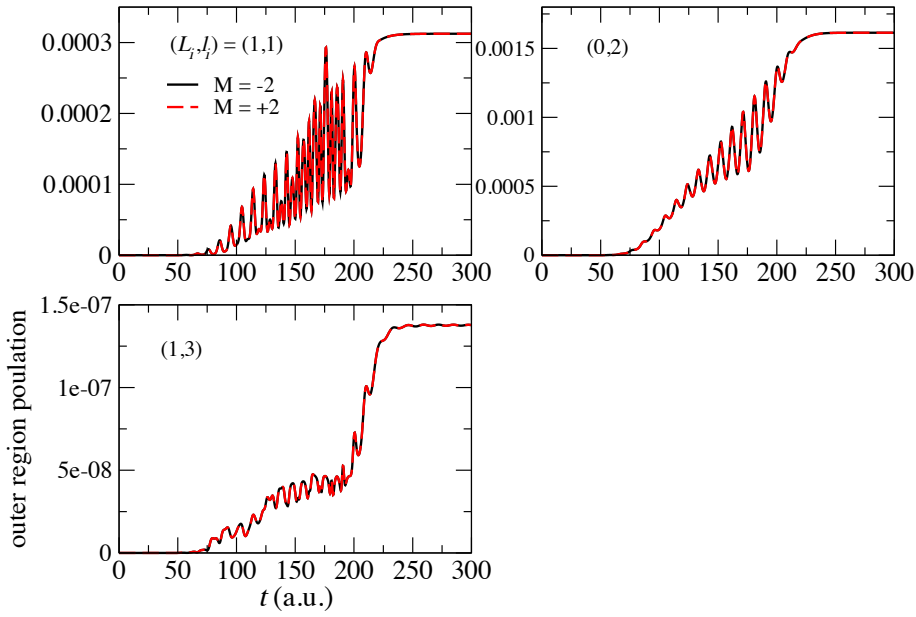


Figure 4: Population in the outer region ($r > 20$ a.u.) for different ${}^1D^e$ channels, for x -axis linear polarization. The values of L_i and l_i are indicated in parentheses.

pathways, as shown in Fig. 5. In this case, we consider one-photon pathways to ${}^1P^o$, and

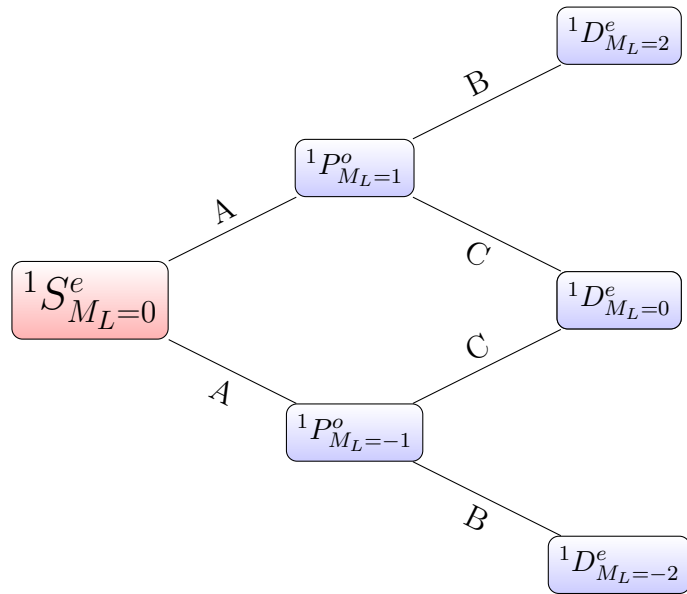


Figure 5: Tree of pathways to each of the magnetic sublevels for ${}^1D^e$ for x -axis linear polarization.

two-photon paths to ${}^1D^e$.

The population in ${}^1P^o_{M_L=-1}$ and ${}^1P^o_{M_L=+1}$ must be equal, as stated earlier. Mathematically, transitions to these states are mediated by equal M_L -dependent Clebsch-Gordan coefficients:

$$A = (0011|11) = (001 - 1|1 - 1) = 1,$$

and hence are equally populated, as indicated by the ‘weight’ label A in Fig. 5. A similar argument holds for the $M_L = \pm 2$ sublevels of ${}^1D^e$, whose population is indicated by B in Fig. 5. Population of this state will be influenced by the Clebsch-Gordan coefficients

$$B = (1111|22) = (1 - 11 - 1|2 - 2) = 1,$$

However, this argument can be used to deduce the branching ratio between these sublevels and the $M_L = 0$ sublevel. Population of the $M_L = 0$ sublevel will be influenced by the Clebsch-Gordan coefficients

$$C = (111 - 1|20) = (1 - 111|20) = \sqrt{\frac{1}{6}},$$

Denoting the transitions to $M_L = 0$ with a weight C in Fig. 5, the population in $M_L = 0$ should be $(2AC)^2$, and the yield in both $M_L = \pm 2$ should be $(AB)^2$. Now the branching ratio for $M_L = 2$ to $M_L = 0$, R_{20} , should be given by

$$R_{20} = \frac{A^2 B^2}{4A^2 C^2} = \frac{B^2}{4C^2} = \frac{1}{\frac{4}{6}} = \frac{3}{2},$$

(167)

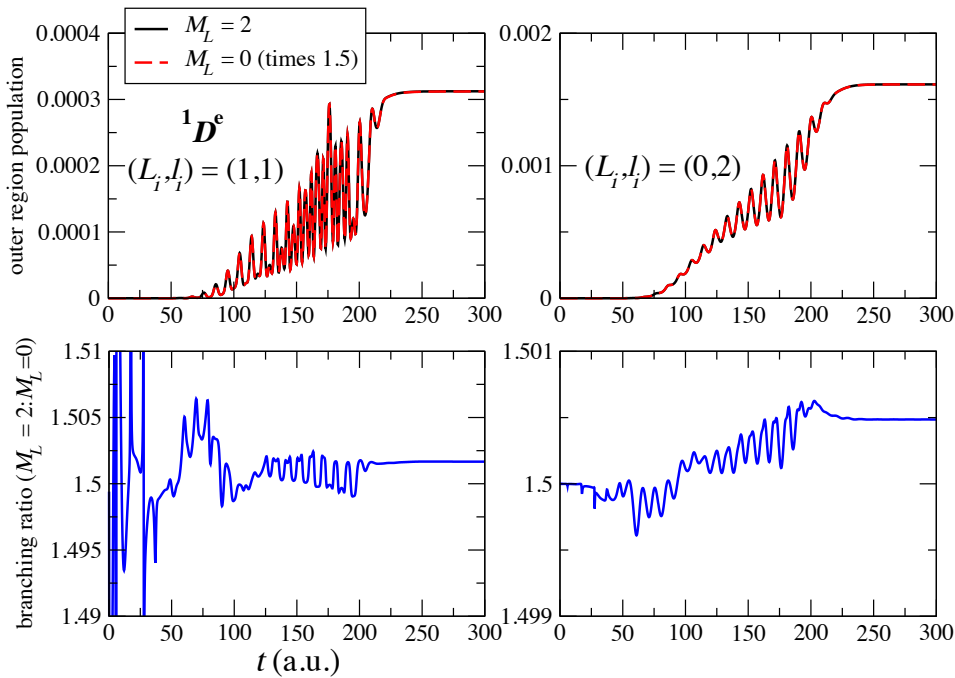


Figure 6: Population in the outer region ($r > 20$ a.u.) for different sublevels of ${}^1D^e$ channels, and the $M_L = 2 : M_L = 0$ branching ratio as a function of time, for x -axis linear polarization. The photon energy is $\omega = 0.33$ a.u.. Note the different scales in each plot. The values of L_i and l_i are indicated in parentheses.

so that the $M_L = -2, 0, 2$ sublevels of ${}^1D^e$ should be populated in the ratio 3:2:3 at all times.

In Fig. 6 we compare outer-region populations for Ar ${}^1D^e$ channels with $M_L = 0$ and $M_L = 2$, for $(L_i, l_i) = (1, 1)$ and $(L_i, l_i) = (0, 2)$. Clearly, when the $M_L = 0$ sublevel yield is increased by a factor of 1.5, it agrees well at all times with the $M_L = 2$ sublevel yield. Plotting the branching ratio as a function of time in each case, we find a near-constant value of 1.5 at all times, with small deviations indicating the level of relative error in the channel populations. In the $(L_i, l_i) = (1, 1)$ case, the branching ratio deviates from 1.5 in the third significant digits, while in the $(L_i, l_i) = (0, 2)$ case, the deviation occurs in the fourth significant digit.

Extending this picture to account for the sublevels of ${}^1F^o$, Fig. 7 shows the 3-photon pathways to the ${}^1F^e$ magnetic sublevels.

Here, we have transitions from $M_L = 2$ to $M_L = 3$ (and from $M_L = -2$ to $M_L = -3$), indicated by the weight factor D , influenced by the 3- j symbols

$$D = (2 - 21 - 1|3 - 3) = (2211|33) = 1.$$

Transitions from $M_L = \pm 2$ to $M_L = \pm 1$ are given weight factor E , and are influence by

$$E = (2 - 211|3 - 1) = (221 - 1|31) = \frac{1}{\sqrt{15}}.$$

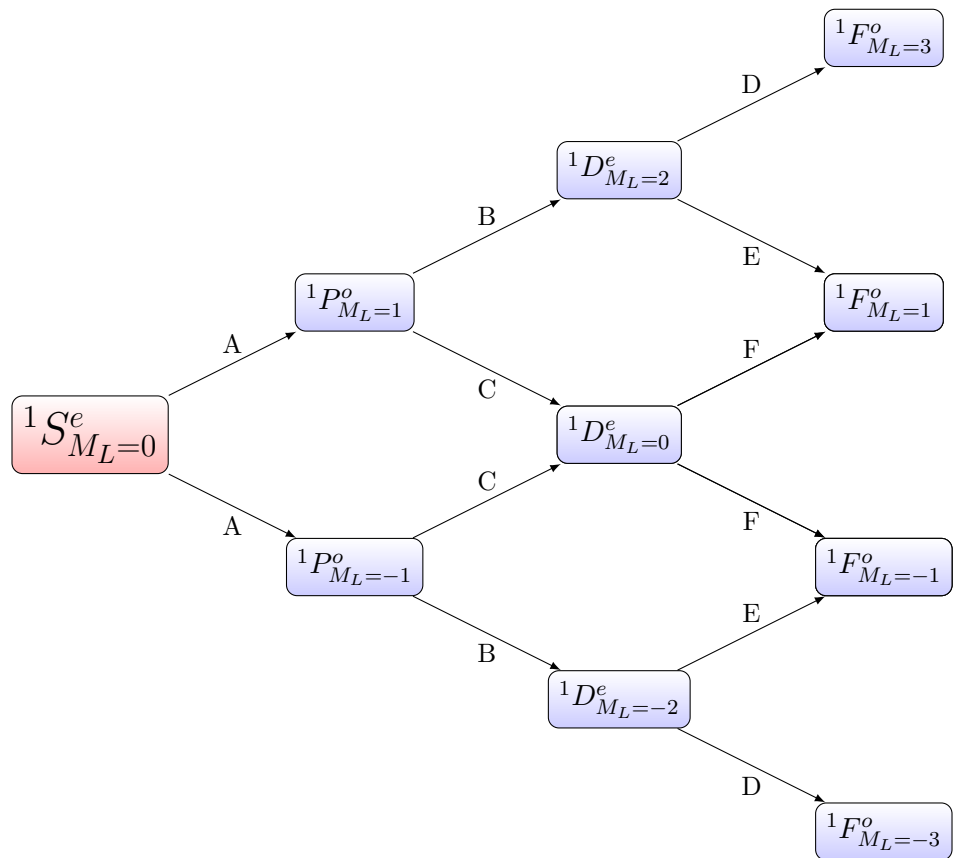


Figure 7: Tree of pathways to each of the magnetic sublevels for ${}^1F^o$ for x -axis linear polarization.

Transitions from $M_L = 0$ to $M_L = \pm 1$ are given weight factor F , and are influence by

$$F = (2011|31) = (201 - 1|3 - 1) = \sqrt{\frac{2}{5}}.$$

From Fig. 7, the relative yields in the $M_L = \pm 3$ sublevels should be $(ABD)^2$, while the yield in $M_L = \pm 1$ should be $(ABE + 2ACF)^2$. Defining R_{31} as the ratio of these quantities, we find that

$$\boxed{R_{31} = \frac{B^2 D^2}{(BE + 2CF)^2} = \frac{1}{\left(\sqrt{\frac{1}{15}} + 2\sqrt{\frac{1}{6}\frac{2}{5}}\right)^2} = \frac{5}{3}.} \quad (168)$$

Fig. 8 shows the outer-region populations and $M_L = 3 : M_L = 1$ branching ratios as a function of time, obtained from a large-scale RMT calculation using a 390-nm pulse. As for the ${}^1D^e$ sublevels of Fig. 6, close agreement is obtained at all times between the $M_L = 3$ sublevel yield and the appropriately scaled $M_L = 1$ sublevel yield. The branching ratios deviate from $\frac{5}{3}$ in the third significant digit once the outer-region populations become significant.

Frame independence

The results given here have been calculated for a particular choice of polarization vector, namely the unit vector along the x -axis. However, it can be shown that the results should hold for any choice of polarization vector in the $x - y$ plane, i.e. for any electric field of the form

$$\mathbf{E}(t) = E_0(t) \cos \omega t \frac{1}{\sqrt{1 + \epsilon^2}} [\hat{\mathbf{x}} + \epsilon \hat{\mathbf{y}}], \quad (169)$$

where ϵ is an adjustable parameter.

To show this, we may convert the Cartesian form of the field to a spherical representation. We find that

$$E_x(x + \epsilon y) = \frac{E_{-1} - E_1}{\sqrt{1 + \epsilon^2}} \frac{1}{2} [(1 + i\epsilon)r_1 - (1 - i\epsilon)r_{-1}]. \quad (170)$$

The spherical components r_1 and r_{-1} now have different ϵ -dependent prefactors, so the tree diagram in Fig. 5 must be modified. The modified diagram is given in Fig. 9.

It is clear from Fig. 9, that the new branching ratio for the sublevels of ${}^1P^o$ (R_{1-1}), previously shown to be equal to one, is now

$$R_{1-1}(\epsilon) = \frac{|1 + i\epsilon|^2 A^2}{|1 - i\epsilon|^2 A^2} = 1. \quad (171)$$

So, for all ϵ , i.e. all linear polarizations in the $x - y$ plane,

$$\boxed{R_{1-1}(\epsilon) = 1.} \quad (172)$$

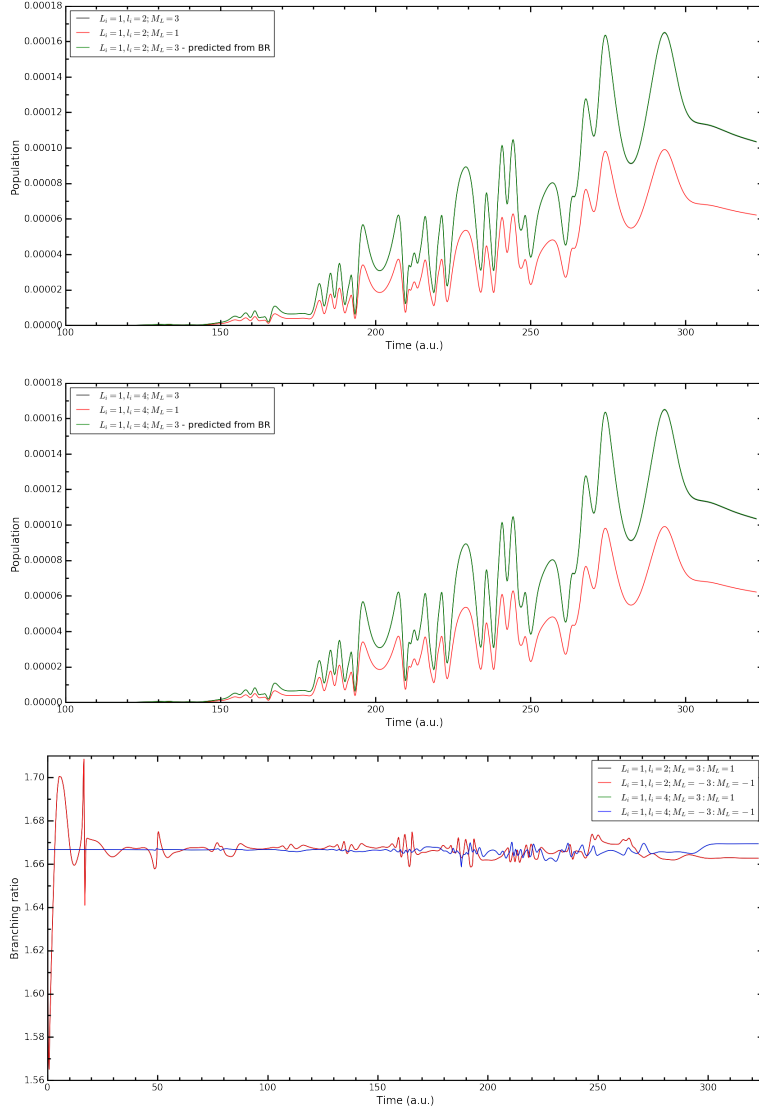


Figure 8: Population in the outer region ($r > 20$ a.u.) for different sublevels of ${}^1F^o$ channels, and the $M_L = 3 : M_L = 1$ branching ratio as a function of time. The photon energy is $\omega = 0.058$ a.u. ($\lambda = 390$ nm).

Similarly, the ϵ -dependent branching ratio R_{20} may be derived. It is now given by

$$R_{20} = \frac{|(1+i\epsilon)A(1+i\epsilon)B|^2}{|-2(1+i\epsilon)(1-i\epsilon)AC|^2} = \frac{|(1+2i\epsilon-\epsilon^2)|^2 B^2}{4(1+\epsilon^2)^2 C^2} = \frac{[(1-\epsilon^2)^2 + 4\epsilon^2]B^2}{4(1+\epsilon^2)^2 C^2} = \frac{B^2}{4C^2}, \quad (173)$$

as before, so for all polarizations in the $x - y$ plane,

$$R_{20}(\epsilon) = \frac{3}{2}.$$

(174)

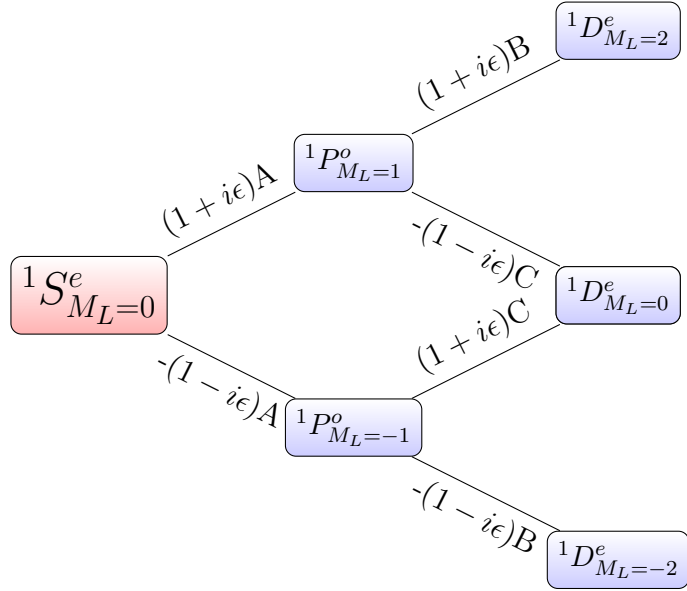


Figure 9: Tree of pathways to each of the magnetic sublevels for ${}^1D^e$ for general linear laser polarization in the $x - y$ plane.

Additionally, the channel populations themselves will be independent of ϵ . Consider the ${}^1P^o_{ML=1}$ channel. For x -axis polarization, its relative population is A^2 . For general polarization in the $x - y$ plane, its population will be

$$\left| \frac{(1 + i\epsilon)A}{\sqrt{1 + \epsilon^2}} \right|^2 = A^2$$

as before. This argument may be extended to all channels, and therefore to the total yield. This is demonstrated in Fig. 11, where RMT calculations demonstrate ϵ -independent population in the outer region.

A.2. Linear polarization in the $(x - z)$ plane

The $(x - z)$ plane provides a perhaps more stringent test of the code, as it allows all possible transitions among magnetic sublevels ($\Delta M_L = 0, \pm 1$) to occur. The electric field is given the form

$$\mathbf{E}(t) = E_0(t) \cos \omega t \frac{1}{\sqrt{1 + \epsilon^2}} [\hat{\mathbf{x}} + \epsilon \hat{\mathbf{z}}], \quad (175)$$

for variable ϵ .

The lowest-order pathways are then given by Fig. 12. In this case, the spherical representation of the dipole interaction takes the form

$$E_x(x + \epsilon z) = E_0 \left[\epsilon r_0 - \frac{1}{\sqrt{2}} (r_{-1} - r_1) \right] = \frac{E_0}{\sqrt{2}} \left[\epsilon \sqrt{2} r_0 + (r_1 - r_{-1}) \right]. \quad (176)$$

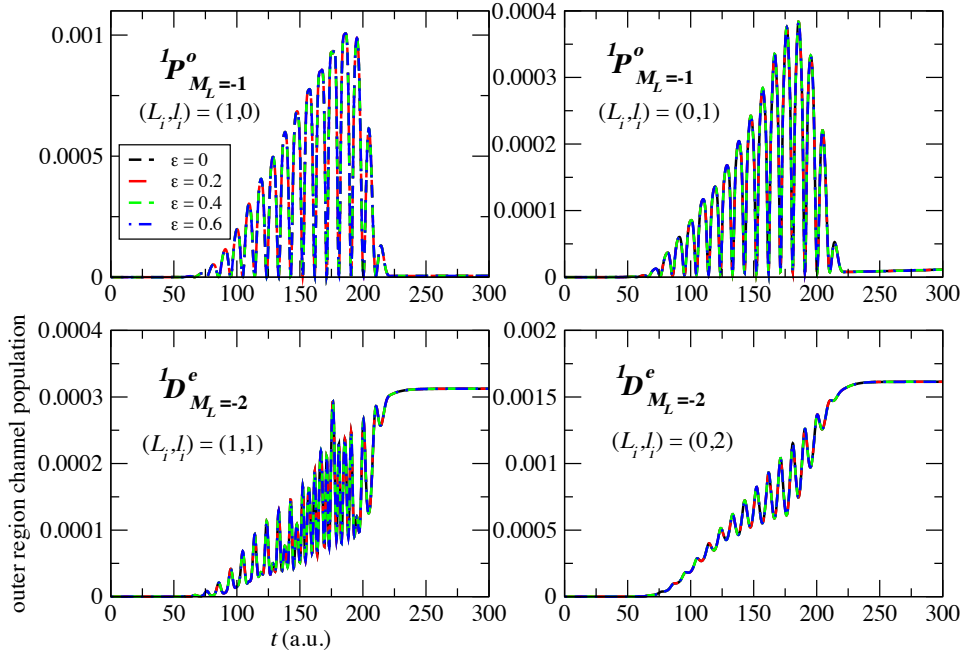


Figure 10: Channel populations in the outer region ($r > 20$ a.u.) for linear polarization of different directions in the $x - y$ plane as a function of time.

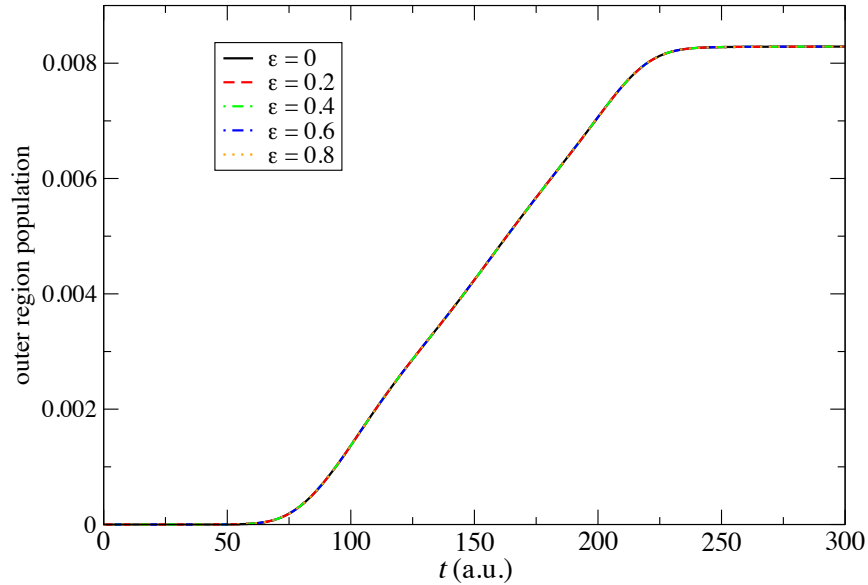


Figure 11: Total population in the outer region ($r > 20$ a.u.) for linear polarization of different directions in the $x - y$ plane.

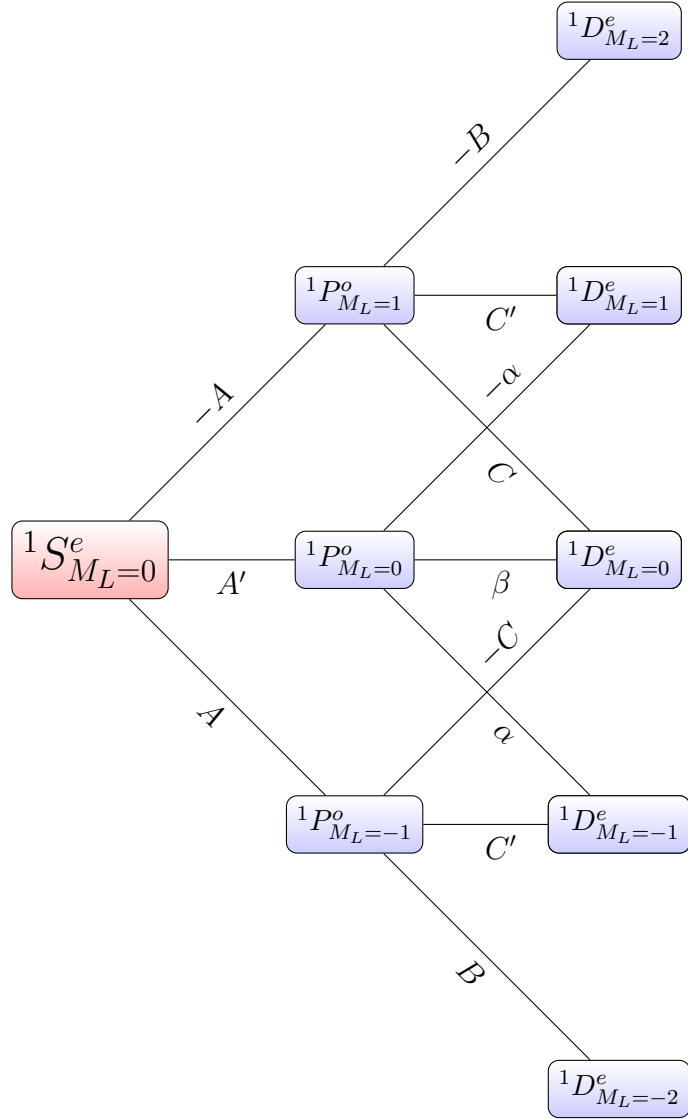


Figure 12: Tree of pathways to each of the magnetic sublevels for ${}^1D^e$ for polarization in the $(x - z)$ plane.

This means that $\Delta M_L = 0$ transitions acquire the opposite sign to $\Delta M_L = +1$ transitions, and the same sign as $\Delta M_L = -1$ transitions (CHECK!!). This is indicated in Fig. 12, where $\Delta M_L = +1$ have been given an additional minus sign. For one-photon transitions to sublevels of ${}^1P^o$, we find that the $\Delta M_L = 0$ transition is influenced by the Clebsch-Gordan coefficient

$$A' = (0010|10) = (0011|11) = 1,$$

and so (weighting A' by a factor of ϵ and $\sqrt{2}$, noting the difference in W_p for x -axis and

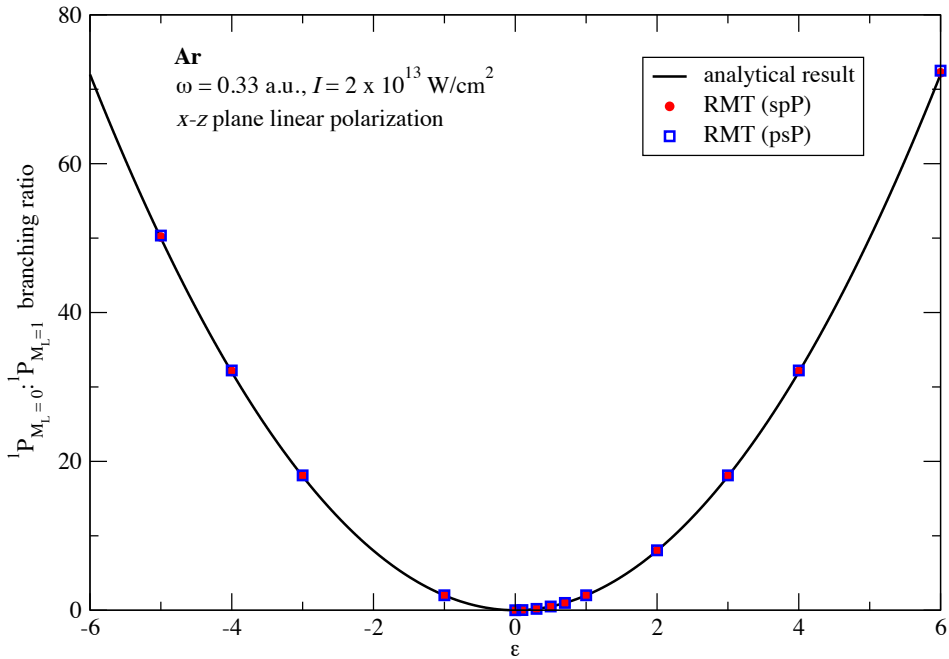


Figure 13: Branching ratios, calculated at the end of the pulse, for sublevels of ${}^1P^o$ as a function of ϵ (different linear polarizations in the $x - z$ plane).

z -axis polarization)

$$R_{01}(\epsilon) = 2\epsilon^2 \left(\frac{A'}{A} \right)^2. \quad (177)$$

Therefore, the branching ratio of the $M_L = 0$ sublevel to the $M_L = 1$ sublevel will be

$$\boxed{R_{01}(\epsilon) = 2\epsilon^2.} \quad (178)$$

This expression, of course, recovers the correct limits as $\epsilon \rightarrow 0$ (x -axis polarization) and $\epsilon \rightarrow \infty$ (z -axis polarization). Explicitly,

$$R_{01}(\epsilon) \rightarrow \begin{cases} 0 & \text{as } \epsilon \rightarrow 0 \\ \infty & \text{as } \epsilon \rightarrow \infty \end{cases}, \quad (179)$$

as expected.

Fig. 13 shows a comparison of the branching ratio of the $M_L = 0$ and $M_L = 1$ sublevels as a function of ϵ , obtained from an RMT calculation (at the end of the laser pulse) with the analytical result in Eq. (178). Clearly, the analytical dependence on ϵ is observed in the calculations, for both $L_i = 0, l_i = 1$ (i.e. spP) and $L_i = 1, l_i = 0$ (i.e. psP).

Similarly, branching ratios among the ${}^1D^e$ sublevels will depend on ϵ . We first consider the $M_L=1:M_L=2$ branching ratio — which of course is always zero for $x - y$ plane polarization.

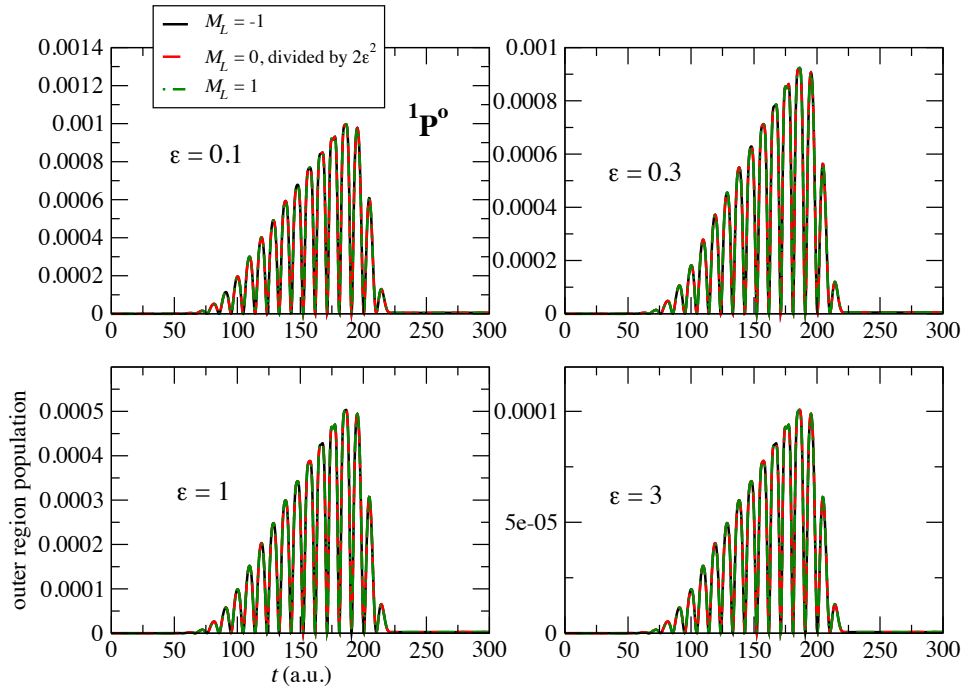


Figure 14: Outer region populations for sublevels of $(L_i = 1, l_i = 0)^1P^o$ as a function of time for different values of ϵ (different linear polarizations in the $x - z$ plane).

The $M_L = 1$ sublevel is now access by two paths, whose weights are indicated in Fig. 12 as $-A'\alpha$ and $-AC'$. C' gives a contribution from z -axis polarization of weight

$$C' = \epsilon\sqrt{2}(1110|21) = \epsilon\sqrt{2}\sqrt{\frac{1}{2}} = \epsilon,$$

Pathways α gives a contribution from z -axis polarization of weight

$$\alpha = (1011|21) = \sqrt{\frac{1}{2}}.$$

So, the $M_L=1:M_L=2$ branching ratio, R_{12} is given by

$$R_{12} = \frac{(-AC' - A'\alpha)^2}{A^2B^2} = \frac{(C' + \epsilon\sqrt{2}\alpha)^2}{B^2} = \frac{\left(\epsilon + \epsilon\sqrt{2}\sqrt{\frac{1}{2}}\right)^2}{1} = 4\epsilon^2, \quad (180)$$

so,

$$R_{12}(\epsilon) = 4\epsilon^2. \quad (181)$$

Again, this recovers the expected branching ratio of 0 when $\epsilon = 0$.

Now for the ${}^1D_{M_L=0}^e$ final states, three paths now occur, two AC paths, and the $A'\beta$ path. Since they both involve one r_1 transition and one r_{-1} transition, they acquire an additional

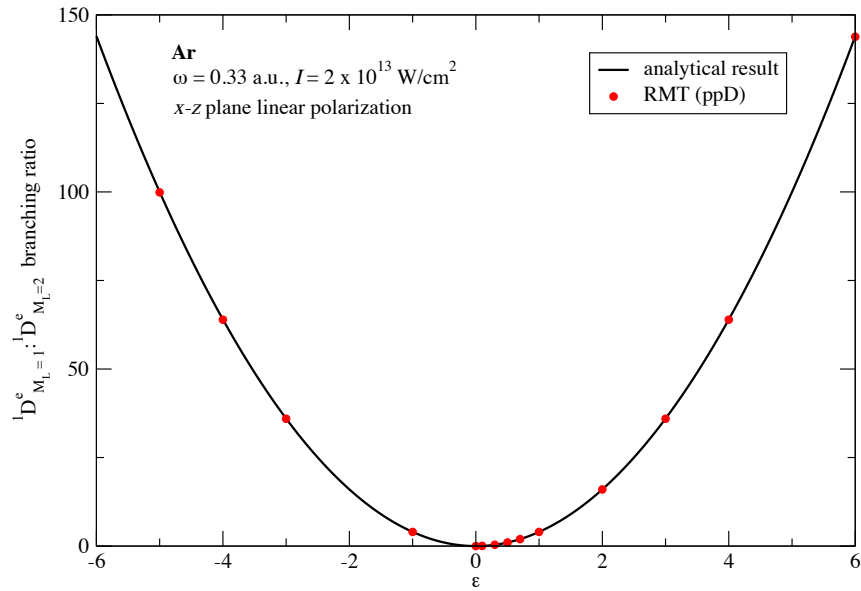


Figure 15: Branching ratios, calculated at the end of the pulse, for sublevels of ${}^1D^e$ as a function of ϵ (different linear polarizations in the $x - z$ plane).

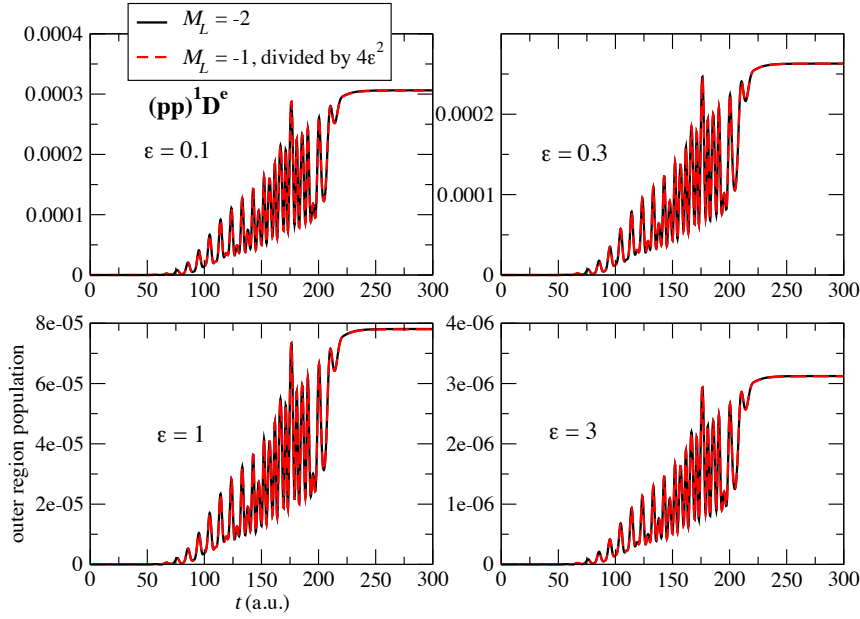


Figure 16: Outer region populations for sublevels of $(L_i = 1, l_i = 1){}^1D^e$ as a function of time for different values of ϵ (different linear polarizations in the $x - z$ plane).

factor of -1. The $A'\beta$ path does not acquire either of these factors since $M_L = 0$ throughout. Therefore, these paths should be combined as $-2AC + (\epsilon\sqrt{2})^2A'\beta = -2A(C - \epsilon^2\beta)$. Now,

β is given by

$$\beta = (1010|20) = \sqrt{\frac{2}{3}},$$

and C was found previously to be $\sqrt{1/6}$. Therefore, we find that the branching ratio for the $M_L = 0$ sublevel to the $M_L = 2$ sublevel is

$$R_{02} = \frac{4A^2(C - \epsilon^2\beta)^2}{A^2B^2} = \frac{4\left(\sqrt{\frac{1}{6}} - \epsilon^2\sqrt{\frac{2}{3}}\right)^2}{1} = \frac{2}{3}(1 - 2\epsilon^2)^2.$$

(182)

Therefore, the sublevels of ${}^1D^e$ should be populated in the ratio

$$3 : 12\epsilon^2 : 2(1 - 2\epsilon^2)^2 : 12\epsilon^2 : 3.$$

Again, for $\epsilon = 0$ the ratio obtained previously for x -axis polarization — 3:0:2:0:3 — is recovered, as expected.

Fig. 15 shows that branching ratio of the $M_L = 1$ sublevel to the $M_L = 2$ sublevel of ${}^1D^e$, calculated at the end of the pulse. The results from RMT calculations are in excellent agreement with the predicted analytical ratio of $4\epsilon^2$.

Fig. 17 shows that branching ratio of the $M_L = 0$ sublevel to the $M_L = 2$ sublevel of ${}^1D^e$, calculated at the end of the pulse. The results from RMT calculations are in excellent agreement with the predicted analytical ratio of $2(1 - 2\epsilon^2)^2/3$. The inset shows that the pronounced minima and maxima at $\epsilon = 0, \pm 1/\sqrt{2}$ are accurately reproduced.

Fig. 18 shows that branching ratio of the $M_L = 1$ sublevel to the $M_L = 0$ sublevel of ${}^1D^e$, calculated at the end of the pulse. The results from RMT calculations are in excellent agreement with the predicted analytical ratio of $6\epsilon^2/(1 - 2\epsilon^2)^2$. Asymptotic behavior near $\epsilon = \pm 1/\sqrt{2}$ is accurately reproduced.

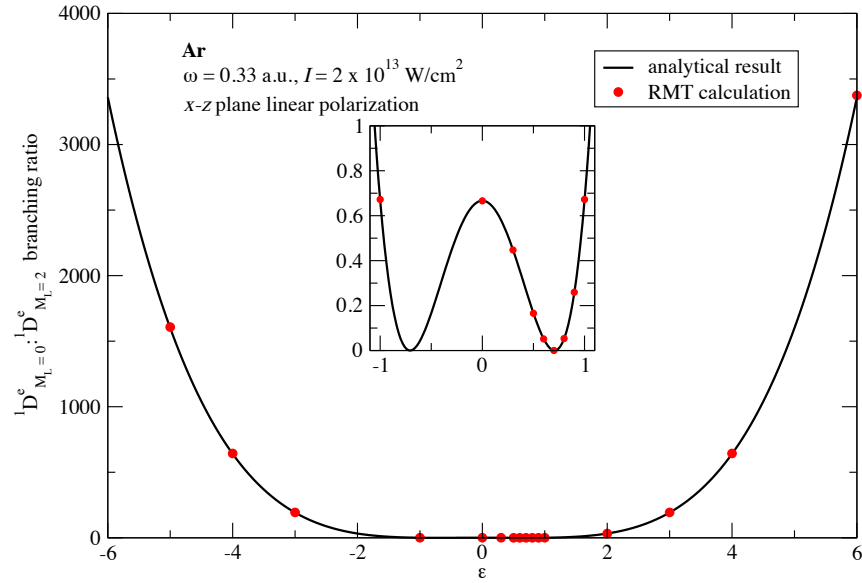


Figure 17: Branching ratios, calculated at the end of the pulse, for sublevels of $^1\text{D}^e$ as a function of ϵ (different linear polarizations in the $x - z$ plane).

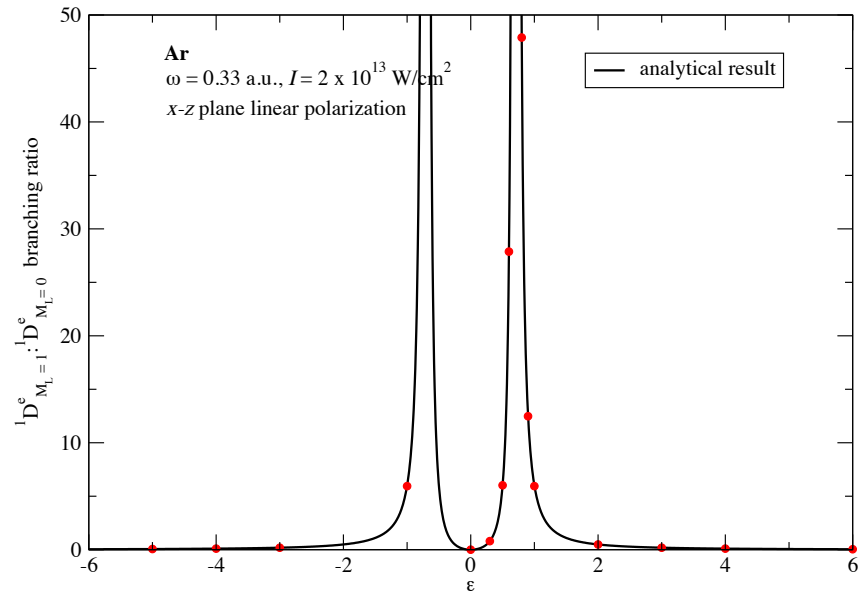


Figure 18: Branching ratios, calculated at the end of the pulse, for sublevels of $^1\text{D}^e$ as a function of ϵ (different linear polarizations in the $x - z$ plane).

A.3. Circular polarization

For circular polarization, the laser field will sweep through all other polarizations in the $x-y$ plane, weighting the positive and negative M_L states differently. However, here the helicity provides a basic check — a helicity of +1 (equivalent to an ellipticity $\epsilon = 1$) should populate positive M_L partial waves as readily as negative helicity populates negative M_L states. In other words, if $\langle M_L \rangle = M$ for $\epsilon = +1$, then $\langle M_L \rangle = -M$ for $\epsilon = -1$.

Fig. 19 shows population in various channels, comparing a given M_L sublevel with $\epsilon = +1$ with its counterpart $-M_L$ sublevel with $\epsilon = -1$.

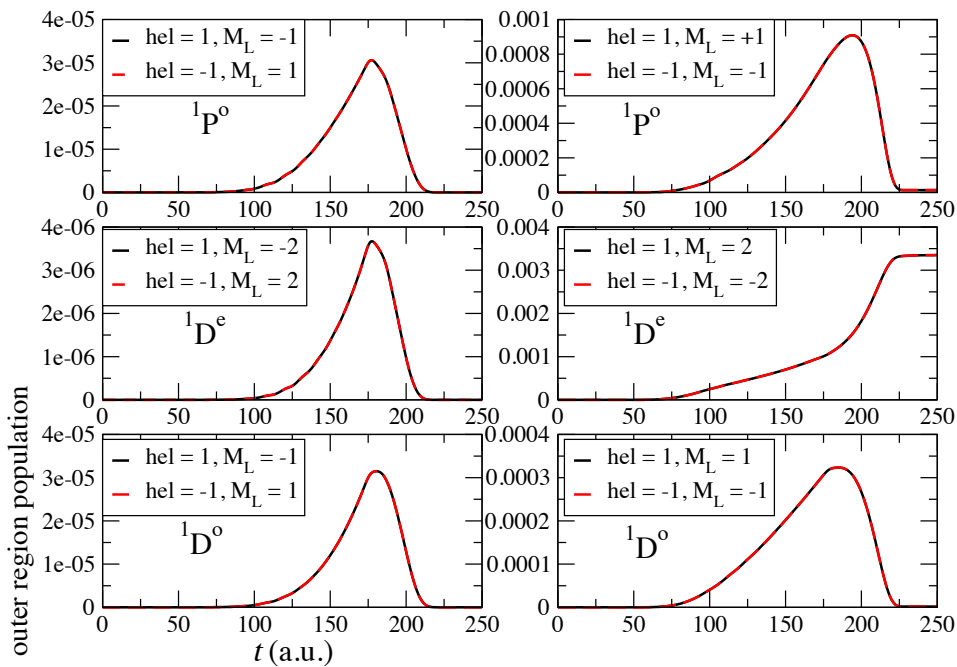


Figure 19: Population in the outer region ($r > 20$ a.u.) of different partial waves for circular polarization of different helicities.

If this is true, then the population in $M_L = 0$ sublevels should be independent of helicity. Fig. 20 shows this for the $M_L = 0$ sublevels of ${}^1S^e$ and ${}^1P^e$, and Fig. 21 shows this for the $M_L = 0$ sublevels of ${}^1D^e$.

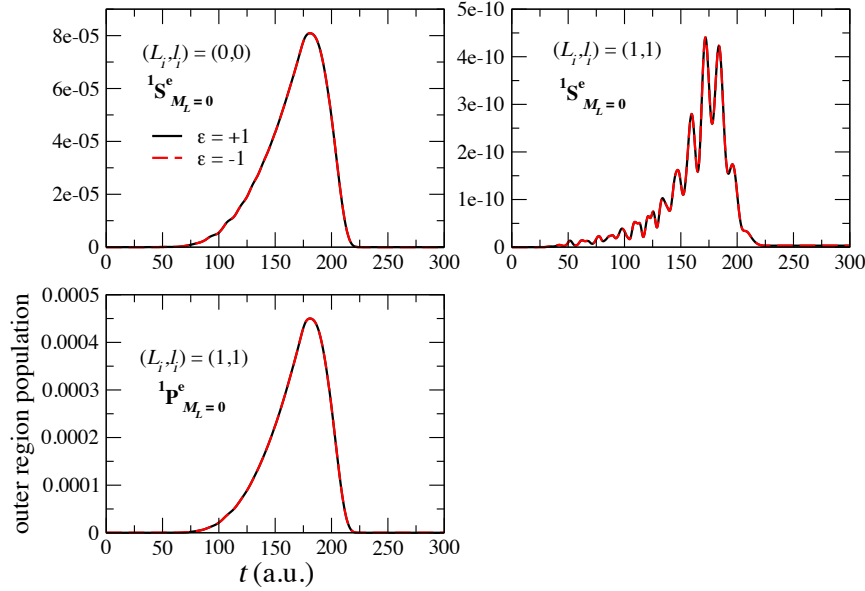


Figure 20: Population in the outer region ($r > 20$ a.u.) of ${}^1S^e$ and ${}^1P^e$ $M_L = 0$ sublevels for circular polarization of different helicities.

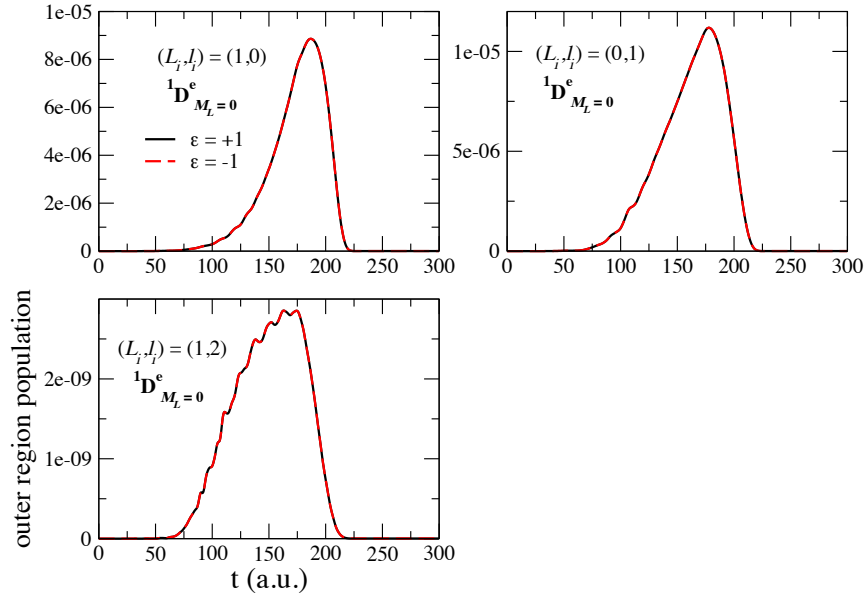


Figure 21: Population in the outer region ($r > 20$ a.u.) of ${}^1D^e$ $M_L = 0$ sublevels for circular polarization of different helicities.

A.4. Elliptical polarization

For elliptical polarization with ellipticity ϵ , we take an electric field of the form

$$\mathbf{E}(t) = \frac{E_0}{\sqrt{1 + \epsilon^2}} (\cos \omega t \hat{\mathbf{x}} + \epsilon \sin \omega t \hat{\mathbf{y}}), \quad (183)$$

for $x - y$ plane polarization, with $E_0 = 0.05336\sqrt{I}$, where I is intensity in units of 10^{14} W/cm^2 .

In an attempt to test the generality of the code, test calculations were performed for a variety of target atoms. Firstly, calculations were performed for an Ar model containing angular momenta $L = 0 - 3$, extending the model for $L = 0 - 2$ used in earlier calculations. In this model, 31 LM_L blocks are required, and so 31 cores are used for the inner region calculation, where 17 were required previously. Comparison was made between the two versions of the RMT suits for arbitrarily-polarized laser fields. Tests were carried out using polarization in both $x - y$ and $x - z$ planes.

B. Boundary tests

Tests were carried out to check that the wavefunction and its derivative were continuous across the inner-region boundary. Fig. 26 shows the real part of $f_p(r, t_f)$ at the final time t_f as a function of r for the $r \leq 40$ a.u. portion of the radial grid. Good continuity is observed across the boundary — the values calculated on the boundary agree to at least 4 digits in all cases shown in Fig. 26, even though the magnitudes are typically less than 10^{-4} .

Fig. 27 shows the real part of $f_p(r, t_f)$ at the final time t_f as a function of r for the $r \leq 40$ a.u. portion of the radial grid. At least 4 digits agreement is obtained in all cases shown in Fig. 27.

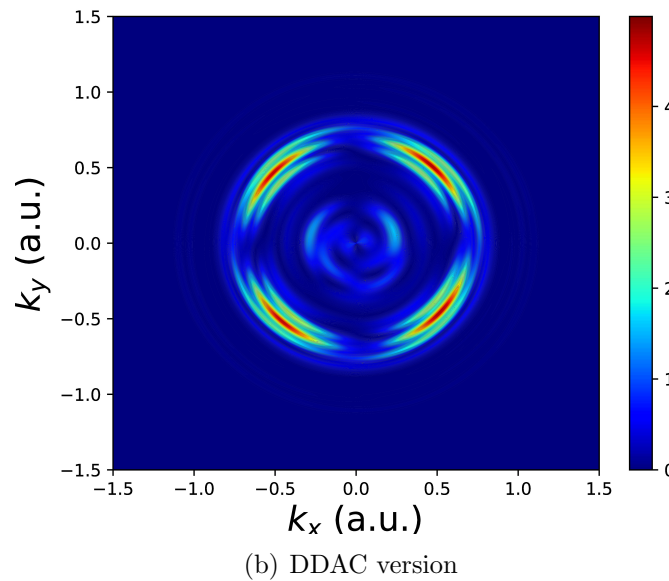
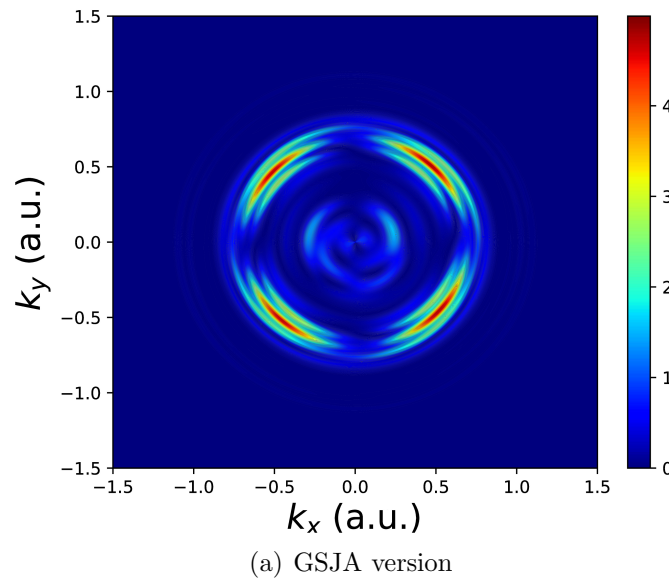


Figure 22: Momentum (p_x, p_y) distribution calculated using both versions of RMT for elliptical polarization. Calculation used the Ar model with $L_{\max} = 2$, and a laser field of intensity 2×10^{13} W/cm², frequency $\omega = 0.33$ a.u., and an ellipticity of $\epsilon = -9$.

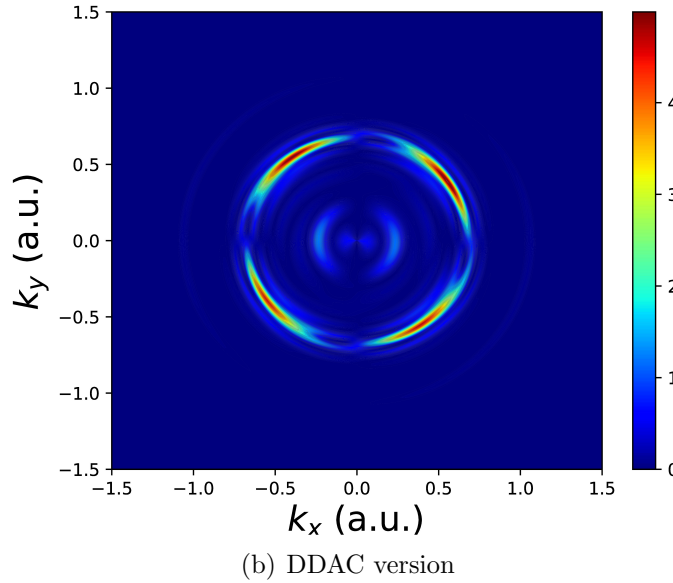
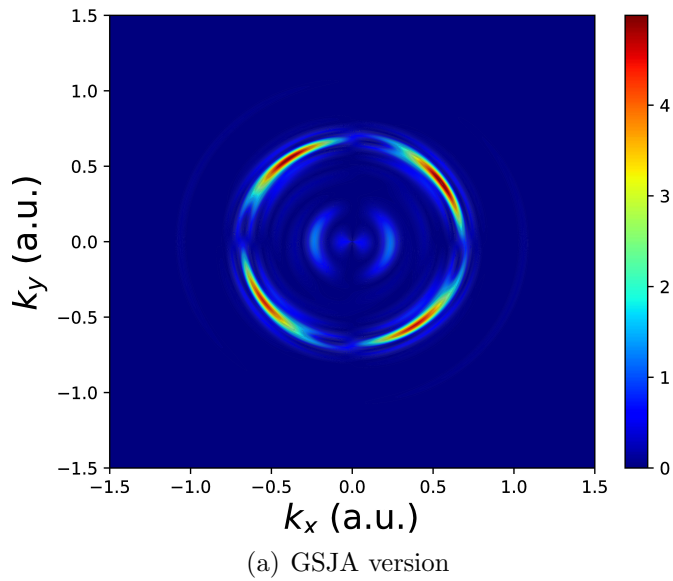


Figure 23: Momentum (p_x, p_y) distribution calculated using both versions of RMT for elliptical polarization. Calculation used the Ar model with $L_{\max} = 2$, and a laser field of intensity 2×10^{13} W/cm², frequency $\omega = 0.33$ a.u., and an ellipticity of $\epsilon = 55$.

XIII. Test case 2: Helium

Helium was used as a test target for an electric field with $\omega = 0.33$ a.u., $I = 2 \times 10^{13}$ W/cm², $T = 12$ cycles, with a 3-cycle ramp-on and ramp-off. This (hopefully!) matches the laser

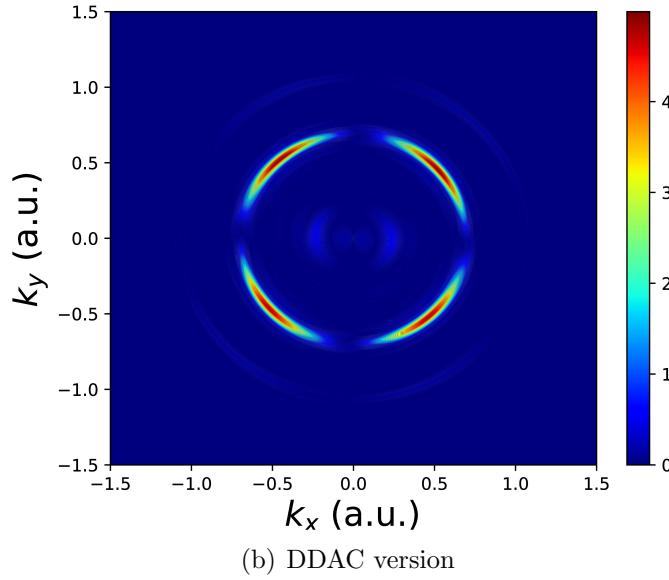
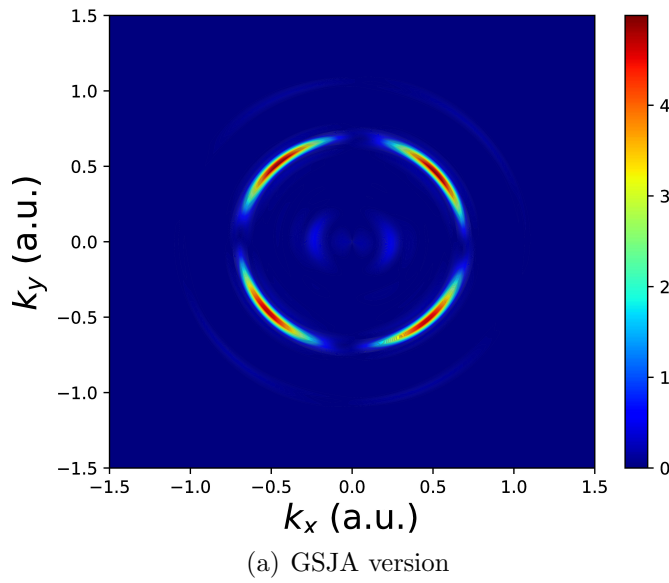


Figure 24: Momentum (p_x, p_y) distribution calculated using both versions of RMT for elliptical polarization. Calculation used the Ar model with $L_{\max} = 2$, and a laser field of intensity 2×10^{13} W/cm², frequency $\omega = 0.33$ a.u., and an ellipticity of $\epsilon = 55$.

pulse used in [5]. Multiple different models were used for the atomic structure calculation using the RMATRXII codes. One model (1T) included only the 1s orbital, another (3P) included the 1s orbital and $\overline{2s}$ and $\overline{2p}$ pseudo-orbitals, and two others (6(P)T) included 3s,3p

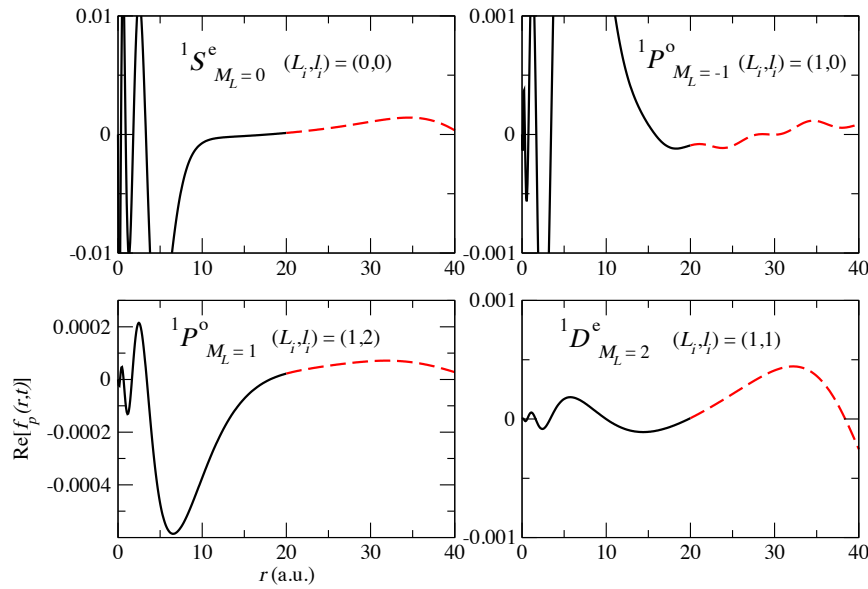


Figure 25: Real part of the ejected-electron wavefunction for different channels as a function of r with an inner region boundary of 20 atomic units.

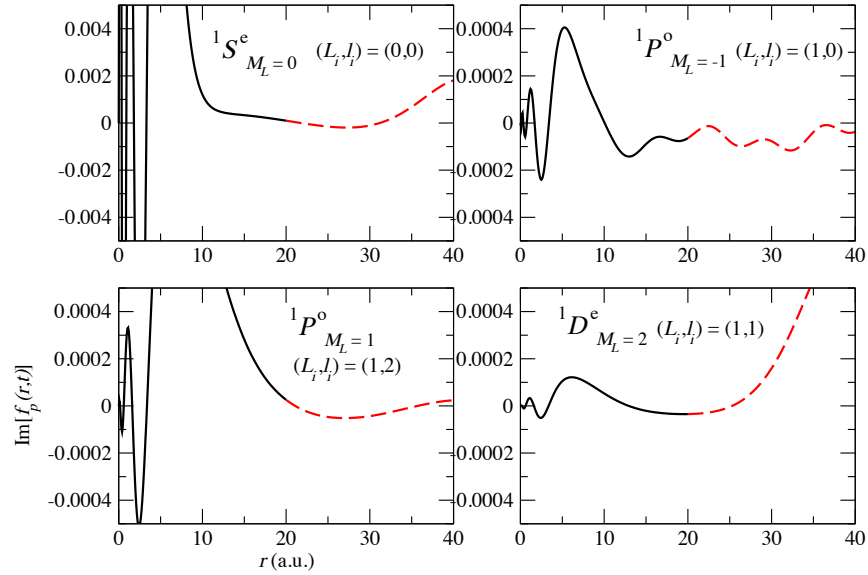


Figure 26: Imaginary part of the ejected-electron wavefunction for different channels as a function of r with an inner region boundary of 20 atomic units.

and 3d (pseudo-)orbitals.

Notably, for stable subsequent propagation in the RMT codes, splines of order $k = 9$ were required in the RAD part of the structure calculation for the 1T and 3P models. When splines

of order 13 were used, the wavefunction norm was not conserved, and rapidly exploded — even after one timestep in some cases! In the 6T and 6P models, stable propagation was achieved with both $k = 9$ and $k = 13$.

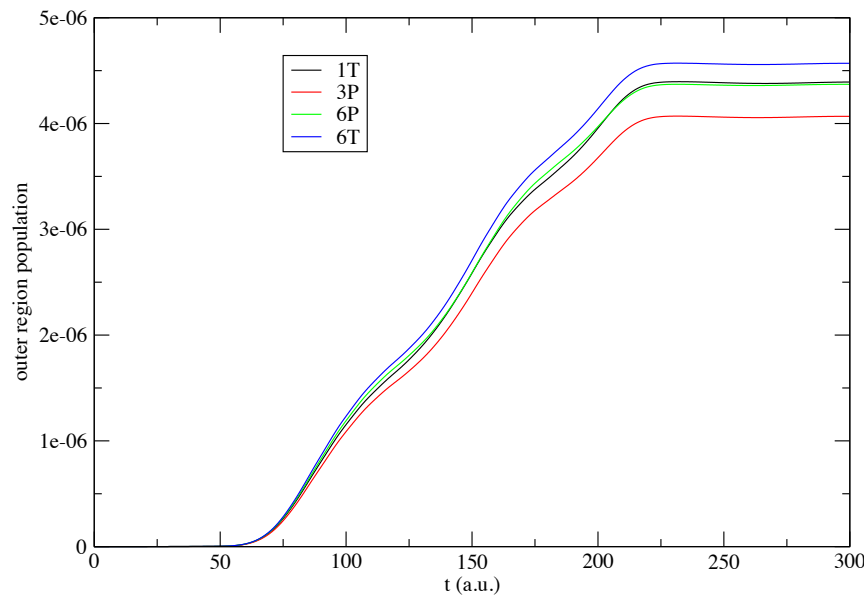


Figure 27: Population in the outer region ($r > 15$ a.u.) for each structure model.

XIV. Code modifications

The existing code for arbitrary polarization was modified to bring it into line with the molecular code. Several changes were implemented. Specific array sizes and indices quoted here refer to the Ar model with $L = 0, 1, 2$, given in table 1.

READHD.f90

1. The logical array `dipole_coupled` array was introduced in READHD.f90. This array of dimension (`No_Of_LML_Blocks`,`No_Of_LML_Blocks`) is a truth table that determines couplings between different LM_L blocks. The array was tested for the Ar test case outlined previously. In this case it is a 17×17 array matching the matrix given in Sec. E..
2. `dipole_coupled` is allocated in the subroutine `Read_D_File`.
3. Values (true/false) are assigned to `dipole_coupled` using loops over `lgmli`,`lgmlf` (i.e. M_L , M'_L), and calls to `finind_new`, which determines a block index for a given LM_L pair. If a pair of blocks `blocki` and `blockf` are coupled, then

$$\text{dipole_coupled}(\text{blocki}, \text{blockf}) = .\text{true}. \quad (184)$$

$$\text{dipole_coupled}(\text{blockf}, \text{blocki}) = .\text{true}. \quad (185)$$

Similarly for coupled (L, L') pairs, the array `dipole_coupled_Lb` keeps track of the indices, so that if `lblocki` couples to `lblockf`,

$$\text{dipole_coupled_Lb}(\text{lblocki}, \text{lblockf}) = .\text{true}. \quad (186)$$

$$\text{dipole_coupled_Lb}(\text{lblockf}, \text{lblocki}) = .\text{true}. \quad (187)$$

4. New array `block_ind(ni,nf)` keeps track of each (L, L') block in order — i.e. it stores the value of `ist` associated with each `(ni,nf)` pair.

DISTRIBUTE HD BLOCKS.f90

1. The `dipole_coupled`, `dipole_coupled_Lb` and `block_ind` arrays are allocated in the (public) subroutine `Allocate_My_Couplings`.
2. The `dipole_coupled`, `dipole_coupled_Lb` and `block_ind` arrays are added to `BCAST_DIPS` and `BCAST_DIPS_RECV`.
3. Array `dsu_mapping` is allocated in the new (public) subroutine `Allocate_dsu_mapping` .
4. Added new routine `Setup_D_Blocks_to_d_s_u_mapping`. In this routine, the array

`dsu_mapping(1:No_Of_LML_Blocks)`

identifies whether a particular (L, L') dipole block is of u , s or d character. The u , s , d blocks are indicated as the numerical values 1,2,3 respectively. Therefore, the u , s , d assignment

is applied to each sublevel coupling within each dipole-coupled (L, L') block. In our case, `dsu_mapping` is set using

$$\text{dsu_mapping}(i) = \begin{cases} 1 & \text{if } L < L' \\ 2 & \text{if } L = L' \\ 3 & \text{if } L > L' \end{cases}, \quad (188)$$

for $i = 1, \text{No_Of_LML_Blocks}$. The value of `dsu_mapping` is then used within `select case` constructs in `Setup_and_distribute_D_Blocks`. Note also that the naming convention in the molecular code differs to that in the atomic code. In the atomic we use the original ordering (u, s, d) to avoid confusion.

5. The new routine `Setup_and_distribute_D_Blocks` is adapted from the molecular code. This routine effectively combines the routines responsible for the setup, sending and receiving of dipole blocks, namely `Setup_And_Send_Dbblocks` and `Recv_Off_Diag_Block_From_Master`, and other called routines. The three main stages, indicated in the code, are:

- **Setup** — Due to the Wigner-Eckardt Theorem, we may factor out the M_L -dependence in the dipole matrix elements, and simply send and receive reduced dipole matrix elements, and multiply by the appropriate Clebsch-Gordan coefficient later. Looping over all rows and columns (`ni` and `nf` i.e. (L, L') blocks), if a row-column pair is coupled, then for all M_L and M'_L , `dblock_12` is assigned as a particular reduced dipole matrix element, accounting for transposition using

```
if (trpse) then
  dblock_12(1:diff_pni,1:diff_pnf) = dipsto(1:diff_pnf,1:diff_pni,ist)
else
  dblock_12(1:diff_pni,1:diff_pnf) = dipsto(1:diff_pni,1:diff_pnf,ist)
endif ,
```

where `ist = block_ind(ni,nf)`, and `trpse = true` if `ist = 0`. In the Ar example,

<code>ist</code>	<code>ni</code>	<code>nf</code>
1	1	3
2	2	3
3	2	5
4	4	3
5	4	5

For all other (ni, nf) pairs, `ist = 0`, and `trpse = .true.` for all other pairs allowed by `dipole_coupled`.

- **Send** — calls to `finind_new` calculate the indices `ni_new` and `nf_new` of the LM_L and $L'M'_L$ blocks. If `ni_new`>1, then `dblock_12` is sent to block master `ni_new`-1. Otherwise, blocks stay with the inner master. The arrays `my_dblock_(u/s/d)` are then assigned using `select case` constructs, using the value of `cnt = dsu_mapping(nf_new)`. For example, for the case `cnt = 1`, `my_dblock_u = dblock_12`. A record of blocks sent is kept in the logical array `blocks_send`, set to true when $(LM_L, L'M'_L)$ blocks are coupled. A record of blocks kept on the master is kept in the logical array `master_blocks`.
- **Receive** — performed for `I_Am_Inner_Master = false`. For all M_L, M'_L , `select case` constructs on `cnt` again dictate which dipole blocks are received. For `cnt = 1`, `my_dblock_u` is received, etc., if `Lb_m_rank = ni_new-1`. A record of blocks received is kept in the logical array `blocks_recv`, set to true when $(LM_L, L'M'_L)$ blocks are coupled. The number of `true` entries in this array is counted later — a warning message is given if this number is not equal to the total number of dipole coupled blocks.

After completing these stages, the code gives a message, stating that each block master has completed construction of the given number of dipole blocks it is responsible for. In the case of the Ar example (see dipole matrix later), block master 0 (inner master) has 3 blocks, block master 1 has 5 blocks, block master 2 has 6 blocks (including the $M_L = M'_L = 0$ block for which the Clebsch-Gordan coefficient is zero) etc..

A further test is performed to ensure that

$$\text{count}(\text{master_blocks}) + \text{count}(\text{blocks_send}) = \text{count}(\text{dipole_coupled}).$$

LIVE_COMMUNICATIONS.f90

1. The new `Setup_Block_Links_New` subroutine sets up the arrays `n_syms_need(1:No.Of_LML_Blocks)` and `wf_syms_need(9,1:No.Of_LML_Blocks)`. The arrays are allocated in `Allocate_my_syms`. This routine also counts the number of u, s and d blocks in a given row of the Hamiltonian.
2.
 - (a) In `Send_Recv_Master_Vecs_Ptp_ZM`, the integer `finast` (used in the molecular code) is replaced with `No.Of_LML_Blocks` for loops over all wavefunction blocks. Block indices are `i` and `j`. The loop over `j = 1,No.Of_LML_Blocks` loops over all block masters.
 - (b) The loop over `k = 1, n_syms_need(j)` loops over the given number of symmetries assigned to a given block master `j` (e.g. `k=1,5` for block master 1, `k=1,6` for block master 2 etc.).
 - (c) The `wf_syms_need` array is then used to locate the position of block number `k` for which block master `j` is responsible. CHECK!!

(d) For this block, `i = wf_syms_need(k, j)`, a vector `my_vec` and an integer `States_Per_LML_Block(i)` are then sent to block master `j-1`. `my_vec` may be `vec_u`, `vec_s` or `vec_d` — the distinction between the cases will be made as they are received, as explained below.

(e) Block masters `j-1` receive a vector `my_vec` and an integer `States_Per_LML_Block`. Their nature is distinguished using `cnt = dsu_mapping(wf_syms_need(k, j))`, which gives values as shown in Eq. (188).

If `cnt = 1`, `my_vec` is received as `vec1`. This is `vec_u`.

If `cnt = 2`, `my_vec` is received as `vec3`. This is `vec_s`.

If `cnt = 3`, `my_vec` is received as `vec2`. This is `vec_d`.

As the vectors are received, their number is counted by the integer `ivecX`, where `X = 1, 3, 2`. A two-dimensional array is created to store the requisite number of vectors. For example, the number of `vec1` vectors received is counted by incrementing `ivec1`. The two-dimensional array `my_vec1s(:, ivec1)=vec1(:)` stores `vec1` for `ivec1 = 1, 2, ...`. These vectors are allocated in `Allocate_my_vecs`, using the values of `no_vecX_init` etc. calculated in `Setup_Block_Links_New`.

If `cnt = 1, 2, 3`, `States_Per_LML_Block` is received as `n_1, n_3, n_2`. These dictate the number of `u, s` and `d` blocks for which matrix vector multiplication will be necessary.

Their values are stored using the arrays `my_blocksizesXs`, where `X = 1, 3, 2`, using for example, `my_blocksizes1s(ivec1) = States_Per_LML_Block(i)` for `ivec1 = 1, 2, ...`.

(f) The Wigner-Eckhardt Theorem is applied, and the Clebsch-Gordan coefficient ($LM_L 1 \Delta M_L |L'M'_L\rangle$) is used (with $\Delta M_L = M'_L - M_L$), and is given as

`cg(lrgl_new(i), 1, lrgl_new(j), ml_new(i), delta_ML, ml_new(j)) .`

The overall factor extracted from the Wigner-Eckardt theorem is given by `cgc`:

$$cgc = (-1)^{L-L'+1} \frac{(LM_L 1 \Delta M_L |L'M'_L\rangle)}{\sqrt{2L'+1}}.$$

The vectors are then multiplied by the appropriate field component, `field(comp)`, with `comp = 2+Delta_ML`, and then by `cgc`.

3. In `Parallel_Matrix_Vector_Multiply_ZM`, the usual calls to `ZGEMV` is performed within loops `ii = 1, N`, where `N = no_vecup, no_vecsame or no_vecdown`, i.e. the required number of `u, s` and `d` blocks. Values of these integers are calculated in `Setup_Block_Links_New`

XV. Issues

A. General

Fourth-order methods used to calculate radials integrals for the wavefunction norm — more accurate than previous lower-order methods.

The boundary point contributes half to the inner region and half to the outer region.

Problems occur if terms involving the Bloch operator (which should cancel) do not cancel. The two Bloch operators act on different wavefunctions, so cancellation is not guaranteed. Non-cancellation results in noticeable deviation from unity in the wavefunction norm.

In the inner region, high-order splines must be included at the boundary, i.e. large-eigenvalue contributions. If these contributions are not included, loss of norm can be observed.

B. Helium

Helium chosen as target for arbitrary-polarization test cases (comparison with Starace vortices). Initial calculations by Daniel gave unphysical populations in the outer region. This may be because the inner region box is to small or too large. The helium ground state is locally confined to a small region of space, $< 10a_0$. So, if an inner region box of around $20a_0$ is used, then there may be a noisy signal at the inner region boundary. This may cause errors when evaluating $H^k\Psi$ if the energy eigenvalue is high, or Lanczos order k is high. Maximum eigenvalue can be lowered by using lower-order splines in inner region — even reduction from say 12 to 8 can help.

However, using a smaller box may also result in an unphysical representation of higher-lying states which extend to larger distances.

XVI. Appendix

A. Matrix elements

A.1. Using 3- j and 6- j symbols

$$\begin{aligned} \langle \alpha_i L_i l_i LM_L | \cos \theta | \alpha'_i L'_i l'_i L' M'_L \rangle &= i^{l'_i - l_i} (-1)^{L + L' + 1 + L_i - M_L} \sqrt{(2L + 1)(2L' + 1)(2l_i + 1)(2l'_i + 1)} \\ &\times \delta_{\alpha_i \alpha'_i} \delta_{L_i L'_i} \delta_{M_L M'_L} \left(\begin{array}{ccc} l_i & 1 & l'_i \\ 0 & 0 & 0 \end{array} \right) \left(\begin{array}{ccc} L & L' & 1 \\ -M_L & M_L & 0 \end{array} \right) \left\{ \begin{array}{ccc} L & L' & 1 \\ l'_i & l_i & L_i \end{array} \right\}, \end{aligned} \quad (189)$$

$$\begin{aligned} \langle \alpha_i L_i l_i LM_L | \sin \theta \cos \phi | \alpha'_i L'_i l'_i L' M'_L \rangle &= i^{l'_i - l_i} (-1)^{L+L'+1+L_i-M_L} \sqrt{\frac{(2L+1)(2L'+1)(2l_i+1)(2l'_i+1)}{2}} \\ &\quad \times \delta_{\alpha_i \alpha'_i} \delta_{L_i, L'_i} \left(\begin{array}{ccc} l_i & 1 & l'_i \\ 0 & 0 & 0 \end{array} \right) \left\{ \begin{array}{ccc} L & L' & 1 \\ l'_i & l_i & L_i \end{array} \right\} \\ &\quad \times \left[\delta_{M'_L, M_L+1} \left(\begin{array}{ccc} L & L' & 1 \\ -M_L & M'_L & -1 \end{array} \right) - \delta_{M'_L, M_L-1} \left(\begin{array}{ccc} L & L' & 1 \\ -M_L & M'_L & 1 \end{array} \right) \right]. \end{aligned} \quad (190)$$

$$\begin{aligned} \langle \alpha_i L_i l_i LM_L | \sin \theta \sin \phi | \alpha'_i L'_i l'_i L' M'_L \rangle &= i^{l'_i - l_i + 1} (-1)^{L+L'+1+L_i-M_L} \sqrt{\frac{(2L+1)(2L'+1)(2l_i+1)(2l'_i+1)}{2}} \\ &\quad \times \delta_{\alpha_i \alpha'_i} \delta_{L_i, L'_i} \left(\begin{array}{ccc} l_i & 1 & l'_i \\ 0 & 0 & 0 \end{array} \right) \left\{ \begin{array}{ccc} L & L' & 1 \\ l'_i & l_i & L_i \end{array} \right\} \\ &\quad \times \left[\delta_{M'_L, M_L+1} \left(\begin{array}{ccc} L & L' & 1 \\ -M_L & M'_L & -1 \end{array} \right) + \delta_{M'_L, M_L-1} \left(\begin{array}{ccc} L & L' & 1 \\ -M_L & M'_L & 1 \end{array} \right) \right]. \end{aligned} \quad (191)$$

$$\begin{aligned} \langle \alpha_i L_i l_i LM_L | \sin \theta e^{\pm i\phi} | \alpha'_i L'_i l'_i L' M'_L \rangle &= \mp i^{l'_i - l_i} (-1)^{L+L'+1+L_i-M_L} \sqrt{2(2L+1)(2L'+1)(2l_i+1)(2l'_i+1)} \\ &\quad \times \delta_{\alpha_i \alpha'_i} \delta_{L_i L'_i} \delta_{M'_L, M_L \mp 1} \left(\begin{array}{ccc} l_i & 1 & l'_i \\ 0 & 0 & 0 \end{array} \right) \left\{ \begin{array}{ccc} L & L' & 1 \\ l'_i & l_i & L_i \end{array} \right\} \left(\begin{array}{ccc} L & L' & 1 \\ -M_L & M'_L & \pm 1 \end{array} \right). \end{aligned} \quad (192)$$

$$\begin{aligned} \langle \alpha_i L_i l_i LM_L | r_\mu^{(1)} | \alpha'_i L'_i l'_i L' M'_L \rangle &= i^{l'_i + 1 - l_i} (-1)^{L+L'+1+L_i-M_L} \sqrt{(2L'+1)(2L+1)(2l'_i+1)(2l_i+1)} \\ &\quad \times \delta_{\alpha_i \alpha'_i} \delta_{L_i L'_i} \delta_{M_L, M'_L + \mu} \left(\begin{array}{ccc} l_i & 1 & l'_i \\ 0 & 0 & 0 \end{array} \right) \left(\begin{array}{ccc} L & L' & 1 \\ -M_L & M'_L & \mu \end{array} \right) \left\{ \begin{array}{ccc} L & L' & 1 \\ l'_i & l_i & L_i \end{array} \right\} r. \end{aligned} \quad (193)$$

A.2. Using Clebsch-Gordan and Racah W coefficients

Alternatively, using Clebsch-Gordan and Racah W coefficients, the general result of Eq. (193) may be written as

$$\begin{aligned} \langle \alpha_i L_i l_i LM_L | r_\mu^{(1)} | \alpha'_i L'_i l'_i L' M'_L \rangle &= i^{l'_i + 1 - l_i} (-1)^{L+L'+1} \delta_{\alpha_i \alpha'_i} \delta_{L_i L'_i} \sqrt{(2L+1)(2l_i+1)} (l_i 010 | l'_i 0) \\ &\quad \times \delta_{M_L, M'_L + \mu} (LM_L 1(-\mu) | L' M'_L) W(1l'_i LL_i, l_i L') r. \end{aligned} \quad (194)$$

Therefore, for example, the $\mu = 0$ ($\cos \theta$) component takes the form (dividing (194) by ir)

$$\begin{aligned} \langle \alpha_i L_i l_i LM_L | \cos \theta | \alpha'_i L'_i l'_i L' M'_L \rangle &= i^{l'_i - l_i} (-1)^{L+L'+1} \delta_{\alpha_i \alpha'_i} \delta_{L_i L'_i} \sqrt{(2L+1)(2l_i+1)} (l_i 010 | l'_i 0) \\ &\quad \times \delta_{M_L M'_L} (LM_L 10 | L' M'_L) W(1l'_i LL_i, l_i L'). \end{aligned} \quad (195)$$

B. Coupling coefficients

$$(j_1 m_1 j_2 m_2 | JM) = (-1)^{j_2 - j_1 - M} \sqrt{2J+1} \begin{pmatrix} j_1 & j_2 & J \\ m_1 & m_2 & -M \end{pmatrix} \quad (196)$$

$$= (-1)^{J-M} \sqrt{2J+1} \begin{pmatrix} j_1 & J & j_2 \\ m_1 & -M & m_2 \end{pmatrix}, \quad (197)$$

$$W(j_1 j_2 J j_3, J_{12} J_{23}) = (-1)^{j_1 + j_2 + j_3 + J} \left\{ \begin{array}{ccc} j_1 & j_2 & J_{12} \\ j_3 & J & J_{23} \end{array} \right\}. \quad (198)$$

C. Shorthands $a(l'_i)$ and $b(l'_i)$

The $a(l'_i)$ term is given by

$$a(l'_i) = -i \langle Y_{l_i 0} | \cos \theta | Y_{l'_i 0} \rangle \quad (199)$$

$$a(l'_i) = - \left\langle Y_{l_i 0} \left| \frac{r_0^{(1)}}{r} \right| Y_{l'_i 0} \right\rangle \quad (200)$$

$$= i^{l'_i - l_i - 1} \sqrt{\frac{2l'_i + 1}{2l_i + 1}} (10l'_i 0 | l_i 0)^2 \quad (201)$$

$$= i^{l'_i - l_i - 1} \sqrt{(2l_i + 1)(2l'_i + 1)} \begin{pmatrix} l_i & 1 & l'_i \\ 0 & 0 & 0 \end{pmatrix}^2, \quad (202)$$

where $l_i = l'_i \pm 1$. The $b(l'_i)$ term is

$$b(l'_i) = \frac{l'_i(l'_i + 1) - l_i(l_i + 1)}{2}, \quad (203)$$

again for $l_i = l'_i \pm 1$.

D. Laplacian commutator

The velocity-gauge laser interaction Hamiltonian is given by ¹

$$H_{\text{int}} = r \left\langle \alpha_i L_i l_i LM_L \left| -\frac{i}{c} \mathcal{A}(t) \frac{\partial}{\partial z} \sum_{p'} \frac{f_{p'}(r, t)}{r} \right| \alpha'_i L'_i l'_i L' M'_L \right\rangle. \quad (204)$$

The z -derivative may be handled using the commutator relation

$$\nabla = \frac{1}{2} [\nabla^2, \mathbf{r}], \quad (205)$$

¹The prefactor of r is used to cancel the $1/r$ term on the LHS, so that it appears as $i \frac{\partial}{\partial t} f_p(R, t)$.

hence

$$\frac{\partial}{\partial z} = \frac{1}{2} [\nabla^2, r \cos \theta]. \quad (206)$$

Therefore

$$H_{\text{int}} = r \sum_{p'} -\frac{i}{2c} \mathcal{A}(t) \left\langle \alpha_i L_i l_i LM_L \left| \nabla^2 (\cos \theta f_{p'}(r, t)) - r \cos \theta \nabla^2 \left(\frac{f_{p'}(r, t)}{r} \right) \right| \alpha'_i L'_i l'_i L' M'_L \right\rangle. \quad (207)$$

The first term in the commutator may be simplified using

$$\begin{aligned} \nabla^2 (\cos \theta f_{p'}(r, t)) |\alpha'_i L'_i l'_i L' M'_L\rangle &= \left[\frac{\partial^2}{\partial r^2} + \frac{2}{r} \frac{\partial}{\partial r} - \frac{\mathbf{l}^2}{r^2} \right] \cos \theta f_{p'}(r, t) |\alpha'_i L'_i l'_i L' M'_L\rangle \\ &= \cos \theta \left[\frac{\partial^2}{\partial r^2} + \frac{2}{r} \frac{\partial}{\partial r} \right] f_{p'}(r, t) |\alpha'_i L'_i l'_i L' M'_L\rangle \\ &\quad - \left[\frac{\mathbf{l}^2}{r^2} \cos \theta \right] f_{p'}(r, t) |\alpha'_i L'_i l'_i L' M'_L\rangle. \end{aligned} \quad (208)$$

The second term in the commutator may be simplified using

$$\begin{aligned} r \cos \theta \nabla^2 \left(\frac{f_{p'}(r, t)}{r} |\alpha'_i L'_i l'_i L' M'_L\rangle \right) &= r \cos \theta \left[\frac{1}{r} \frac{\partial^2}{\partial r^2} - \frac{\mathbf{l}^2}{r^3} \right] f_{p'}(r, t) |\alpha'_i L'_i l'_i L' M'_L\rangle \\ &= \cos \theta \left[\frac{\partial^2}{\partial r^2} - \frac{\mathbf{l}^2}{r^2} \right] f_{p'}(r, t) |\alpha'_i L'_i l'_i L' M'_L\rangle. \end{aligned} \quad (209)$$

Therefore

$$\left[\nabla^2, r \cos \theta \right] \frac{f_{p'}(r, t)}{r} |\alpha'_i L'_i l'_i L' M'_L\rangle = \frac{1}{r} \left[2 \cos \theta \frac{\partial}{\partial r} + \frac{\cos \theta \mathbf{l}^2 - \mathbf{l}^2 \cos \theta}{r} \right] f_{p'}(r, t) |\alpha'_i L'_i l'_i L' M'_L\rangle, \quad (210)$$

and so Eq.(207) becomes

$$\begin{aligned} H_{\text{int}} &= \sum_{p'} -\frac{i}{2c} \mathcal{A}(t) \langle \alpha_i L_i l_i LM_L | \cos \theta |\alpha'_i L'_i l'_i L' M'_L\rangle 2 \frac{\partial}{\partial r} f_{p'}(r, t) \\ &\quad + \sum_{p'} -\frac{i}{2c} \mathcal{A}(t) \langle \alpha_i L_i l_i LM_L | \cos \theta \mathbf{l}^2 |\alpha'_i L'_i l'_i L' M'_L\rangle \frac{f_{p'}(r, t)}{r} \\ &\quad - \sum_{p'} -\frac{i}{2c} \mathcal{A}(t) \langle \alpha_i L_i l_i LM_L | \mathbf{l}^2 \cos \theta |\alpha'_i L'_i l'_i L' M'_L\rangle \frac{f_{p'}(r, t)}{r}. \end{aligned} \quad (211)$$

Now

$$\begin{aligned} \langle \alpha_i L_i l_i LM_L | \mathbf{l}^2 \cos \theta |\alpha'_i L'_i l'_i L' M'_L\rangle &= \langle \alpha'_i L'_i l'_i L' M'_L | \cos \theta \mathbf{l}^2 | \alpha_i L_i l_i LM_L \rangle \\ &= l_i(l_i + 1) \langle \alpha'_i L'_i l'_i L' M'_L | \cos \theta | \alpha_i L_i l_i LM_L \rangle, \\ &= l_i(l_i + 1) \langle \alpha_i L_i l_i LM_L | \cos \theta | \alpha'_i L'_i l'_i L' M'_L \rangle, \end{aligned} \quad (212)$$

and so

$$H_{\text{int}} = \sum_{p'} -\frac{i}{c} \mathcal{A}(t) \langle \alpha_i L_i l_i L M_L | \cos \theta | \alpha'_i L'_i l'_i L' M'_L \rangle \left[\frac{\partial}{\partial r} + \frac{l'_i(l'_i + 1) - l_i(l_i + 1)}{2r} \right] f_{p'}(R, t). \quad (213)$$

E. Hamiltonian structure

For linear polarization along the z -axis, the Hamiltonian has the familiar tridiagonal structure. Transitions can be made for $L' = L, L \pm 1$, i.e. coupling states above and below (in L) the initial state, and states of the same L . The wavefunction vector contains a 3-component chunk, with Upper (U), same (S) and Down (D) components, for example, when making transitions from a ${}^1F^o$ state:

$$\Psi = \begin{pmatrix} \vdots \\ \vdots \\ {}^1D^e \\ \vdots \\ {}^1F_o \\ \vdots \\ {}^1G^e \\ \vdots \end{pmatrix} = \begin{pmatrix} \vdots \\ \vdots \\ U \\ S \\ D \\ \vdots \\ \vdots \end{pmatrix} \quad (214)$$

For linear polarization along the z axis, with $M_L = 0$, the Hamiltonian takes the usual form

$$\begin{pmatrix} {}^1S^e & {}^1P^o & {}^1D^e & {}^1F^o & {}^1G^e \\ & D & & & \\ U & & D & & \\ & U & & D & \\ & & U & & D \\ & & & U & \end{pmatrix} \begin{pmatrix} {}^1S^e \\ {}^1P^o \\ {}^1D^e \\ {}^1F^o \\ {}^1G^e \end{pmatrix}$$

Dipole blocks are then given as `my_dblock_u`, `my_dblock_s` and `my_dblock_d`.

Now including $M_L \in [-L, L]$, the Hamiltonian becomes

$$\begin{pmatrix} {}^1S^e & {}^1P_{-1}^e & {}^1P_0^e & {}^1P_1^e & {}^1P_{-1}^o & {}^1P_0^o & {}^1P_1^o \\ & & & & D & D & D \\ & & & & S & S & \\ & & & & S & & S \\ & & & & & S & S \\ U & S & S & & & & \\ U & S & & S & & & \\ U & & S & S & & & \end{pmatrix} \begin{matrix} {}^1S^e \\ {}^1P_{-1}^e \\ {}^1P_0^e \\ {}^1P_1^e \\ {}^1P_{-1}^o \\ {}^1P_0^o \\ {}^1P_1^o \end{matrix}$$

E.1. Ar model

Now for the Ar model with $L_{\max} = 2$,

Channel ID	LM_L Block	$L_i l_i L$	$LM_L SII$
1	1	000	$^1S_{M_L=0}^e$
2	1	110	
3	2	111	$^1P_{M_L=-1}^e$
4	3	111	$^1P_{M_L=0}^e$
5	4	111	$^1P_{M_L=1}^e$
6	5	101	
7	5	011	$^1P_{M_L=-1}^o$
8	5	121	
9	6	101	
10	6	011	$^1P_{M_L=0}^o$
11	6	121	
12	7	101	
13	7	011	$^1P_{M_L=1}^o$
14	7	121	
15	8	112	
16	8	022	$^1D_{M_L=-2}^e$
17	8	132	
18	9	112	
19	9	022	$^1D_{M_L=-1}^e$
20	9	132	
21	10	112	
22	10	022	$^1D_{M_L=0}^e$
23	10	132	
24	11	112	
25	11	022	$^1D_{M_L=1}^e$
26	11	132	
27	12	112	
28	12	022	$^1D_{M_L=2}^e$
29	12	132	
30	13	212	$^1D_{M_L=-2}^o$
31	14	212	$^1D_{M_L=-1}^o$
32	15	212	$^1D_{M_L=0}^o$
33	16	212	$^1D_{M_L=1}^o$
34	17	212	$^1D_{M_L=2}^o$

Table 1: Channel ID for Ar structure model

the dipole matrix takes the form

$^1S^e$	$^1P_{-1}^e$	$^1P_0^e$	$^1P_1^e$	$^1P_{-1}^o$	$^1P_0^o$	$^1P_1^o$	$^1D_{-2}^e$	$^1D_{-1}^e$	$^1D_0^e$	$^1D_1^e$	$^1D_2^e$	$^1D_{-2}^o$	$^1D_{-1}^o$	$^1D_0^o$	$^1D_1^o$	$^1D_2^o$
				D	D	D										$^1S^e$
				S	S							D	D	D		$^1P_{-1}^e$
				S		S						D	D	D		$^1P_0^e$
				S	S							D	D	D		$^1P_1^e$
U	S	S					D	D	D							$^1P_{-1}^o$
U	S		S				D	D	D							$^1P_0^o$
U		S	S				D	D	D							$^1P_1^o$
				U								S	S			$^1D_{-2}^e$
				U	U							S	S	S		$^1D_{-1}^e$
				U	U	U						S		S		$^1D_0^e$
				U	U							S	S	S		$^1D_1^e$
					U							S	S			$^1D_2^e$
	U						S	S								$^1D_{-2}^o$
	U	U					S	S	S							$^1D_{-1}^o$
	U	U	U				S		S							$^1D_0^o$
	U	U					S	S	S							$^1D_1^o$
		U					S	S				S	S			$^1D_2^o$

REFERENCES

- [1] M. A. Lysaght, P. G. Burke and H. W. van der Hart, *Phys. Rev. A* **79** 053411 (2009).
- [2] R. N. Zare, *Angular Momentum* (Wiley) (1987).
- [3] K. J. Meharg *et al.*, *J. Phys. B: At. Mol. Opt. Phys.* **38** 237 (2005).
- [4] P. G. Burke and K. A. Berrington, *Atomic and molecular processes: an R-matrix approach* (1991).
- [5] S. Hutchinson, M. A. Lysaght and H. W. van der Hart, *J. Phys. B: At. Mol. Opt. Phys.* **43** 095603 (2010).
- [6] G. S. J. Armstrong, Y. Wang and B. D. Esry, *Phys. Rev. A* **96** XXXXXX (2016).
- [7] C. de Boor, *A Practical Guide to Splines* (Berlin: Springer) (1978).
- [8] P. Lambropoulos, P. Maragakis and J. Zhang, *Phys. Rep.* **305** 203 (1998).
- [9] F. Martin, *J. Phys. B: At. Mol. Opt. Phys.* **32** R197 (1999).
- [10] H. Bachau, E. Cormier, P. Decleva, J. E. Hansen and F. Martín, *Rep. Prog. Phys.* **64** 1815 (2001).
- [11] X. Tang, H. Rudolph and P. Lambropoulos, *Phys. Rev. Lett.* **65** 3269 (1990).
- [12] E. Cormier and P. Lambropoulos, *J. Phys. B: At. Mol. Opt. Phys.* **30** 77 (1997).
- [13] B. D. Esry, *Ph.D. thesis*, University of Colorado (1997).
- [14] B. D. Esry and H. Sadeghpour, *Phys. Rev. A* **60** 3604 (1999).
- [15] X. Guan, O. Zatsarinny, K. Bartschat, B. I. Schneider, J. Feist and C. J. Noble, *Phys. Rev. A* **76** 053411 (2007).
- [16] M. A. Lysaght, H. W. van der Hart and P. G. Burke, *Phys. Rev. A* **79** 053411 (2009).
- [17] B. H. Branden and C. J. Joachain, *Physics of Atoms and Molecules* (Prentice Hall) (2003).
- [18] E. Cormier and P. Lambropoulos, *J. Phys. B: At. Mol. Opt. Phys.* **29** 1667 (1995).